Preclinical Development of an AAV8-hUGT1A1 Vector for the Treatment of Crigler-Najjar Syndrome

Fanny Collaud, Giulia Bortolussi, Laurence Guianvarc'H, Sem Aronson, Thierry Bordet, Philippe Veron, Severine Charles, Patrice Vidal, Marcelo Simon Sola, Stephanie Rundwasser, et al.

Preclinical development of an AAV8-hUGT1A1 vector for the treatment of Crigler-Najjar syndrome

Fanny Collaud[1#], Giulia Bortolussi[2#], Laurence Guianvarc'h[1#], Sem J. Aronson[3], Thierry Bordet[4], Philippe Veron[1], Severine Charles[1], Patrice Vidal[1], Marcelo Simon Sola[1], Stephanie Rundwasser[1], Delphine G. Dufour[1], Florence Lacoste[1], Cyril Luc[1], Laetitia v. Wittenberghe[1], Samia Martin[1], Christine Le Bec[1], Piter J. Bosma[3], Andres F. Muro[2], Giuseppe Ronzitti[1], Matthias Hebben[1], Federico Mingozzi[1 †]

[1] INTEGRARE, Genethon, Inserm, Univ Evry, Université Paris-Saclay, 91002, Evry, France

[2]International Center for Genetic Engineering and Biotechnology, 34149 Trieste, Italy

[3,]Amsterdam UMC, University of Amsterdam, Tytgat Institute for Liver and Intestinal Research, AG&M, 1105 BK Amsterdam, the Netherlands

[4]AFM-Telethon, 91000, Evry, France

# These authors contributed equally

[†] on behalf of the CureCN consortium

Short title: AAV gene therapy for Crigler-Najjar syndrome.

Corresponding author:

Federico Mingozzi, PhD

1 rue de l'Internationale, 91000 Evry, France

fmingozzi@genethon.fr

ABSTRACT

Adeno-associated viruses (AAV) are among the most efficient vectors for liver gene therapy. Results obtained in the first hemophilia clinical trials demonstrated the long-term efficacy of this approach in humans, showing efficient targeting of hepatocytes with both self-complementary (sc) and single-stranded (ss) AAV vectors. However, to support clinical development of AAV-based gene therapies, efficient and scalable production processes are needed. In an effort to translate to the clinic an approach of AAV-mediated liver gene transfer to treat Crigler-Najjar (CN) syndrome, we developed a (ss)AAV8 vector carrying the human UDP-glucuronosyltransferase- family 1-member A1 (hUGT1A1) transgene under the control of a liver-specific promoter. We compared our construct with similar (sc)AAV8 vectors expressing hUGT1A1, showing comparable potency in vitro and in vivo. Conversely, (ss)AAV8-hUGT1A1 vectors showed superior yields and product homogeneity compared with their sc counterpart. We then focused our efforts in the scale-up of a manufacturing process of the clinical product (ss)AAV8-hUGT1A1 based on the triple-transfection of human embryonic kidney (HEK) 293 cells grown in suspension. Large-scale production of this vector had characteristics identical to those of small-scale vectors produced in adherent cells. Preclinical studies in animal models of the disease and a good laboratory practice (GLP) toxicology/biodistribution study were also conducted using large scale preparations of vectors. These studies demonstrated long-term safety and efficacy of gene transfer with (ss)AAV8-hUGT1A1 in relevant animal models of the disease, thus supporting the clinical translation of this gene therapy approach for the treatment of CN syndrome.

INTRODUCTION

Crigler-Najjar (CN) syndrome is a rare and severe condition that affects bilirubin metabolism [1, 2]. The disease is due to mutations in the liver-specific enzyme uridine diphosphate glucuronosyltransferase 1A1 (UGT1A1) that conjugates bilirubin and mediates its disposal. The lack of this enzyme results in the accumulation of unconjugated bilirubin in serum, which is associated with brain toxicity and early death [3]. CN syndrome is an inherited autosomal recessive disorder with an incidence of about 1 in 1 000 000 newborns. Therapy for CN syndrome consists of daily cycles of 12-16 hours of exposure to blue light, which results in bilirubin photoisomerization and elimination in the urine. However, poor compliance to phototherapy and loss of efficacy associated with aging, expose patients to potentially lethal bilirubin spikes [3, 4]. At present, there is no authorized medicinal product for treatment of CN syndrome and orthotopic liver transplantation is the only curative treatment, with all the limitations of the approach [3-6].

The monogenic etiology of the disease, the absence of liver parenchymal damage, and the low levels of UGT1A1 enzyme activity needed to correct the phenotype [7], make CN syndrome an ideal target for gene therapy [8, 9]. Adeno-associated virus (AAV) vector-mediated gene therapy is one of the most promising approaches for safe and efficient gene transfer to the liver [10]. The efficacy of liver-directed AAV gene therapy is demonstrated by the recent successes in patients suffering from hemophilia A and B [11-15] and by the growing number of clinical trials using AAV vectors to transfer therapeutic transgenes to the liver.

Several studies showed therapeutic efficacy following AAV vector mediated gene transfer to the liver in both mouse and rat models of CN syndrome [16-20] . Accordingly, we recently showed long-term correction of bilirubin levels following liver-directed gene transfer with an AAV8 vector expressing a codon-optimized version of the UGT1A1 cDNA [21].

However, one of the biggest challenges for the clinical translation of AAV vector-based therapies is vector production. In particular, scalable production systems able to deliver high-

yield and high-purity material are needed [22]. Several AAV vector production platforms have been used to produce clinical-grade vector lots, although in recent years the field coalesced around transfection- and baculovirus- based production methods [23].

Here, in an effort to develop and translate to the clinic a gene therapy for CN syndrome, we developed an AAV8 vector to efficiently express the human UGT1A1 transgene in hepatocytes. We initially compared single-stranded (ss) and self-complementary (sc) AAV vector genome configurations, showing a nearly identical potency profile *in vitro* and *in vivo*. However, based on the yields in production and the impurities profile, we focused production scale up and preclinical studies on a single-stranded AAV8-hUGT1A1 vector. A bioreactor system for the triple transfection human embryonic kidney (HEK)293 cells grown in suspension was established. Dose finding studies were conducted in two animal models of the CN syndrome using full-scale vector preparations. In parallel, good laboratory practice (GLP) studies were performed to evaluate toxicity, vector shedding, and biodistribution of the clinical vector (ss)AAV8-hUGT1A1 in wild-type rats. Germline transmission studies were also performed, together with a detailed assessment of immunogenicity of the therapeutic product. These results support the initiation of a phase I/II clinical trial in patients (ClinicalTrials.gov ID# NCT03466463).

RESULTS

(ss)AAV8-hUGT1A1 vector preparations present better yields and higher product homogeneity compared to (sc)AAV8-hUGT1A1 vectors

We compared (sc)AAV and (ss)AAV vectors encoding for hUGT1A1 under the transcriptional control of liver specific promoters (Figure 1A). The two expression cassettes were pseudotyped into AAV serotype 8 to efficiently transduce the liver of animals [12, 24]. Research grade vector preparations were obtained by triple transfection of adherent HEK293 cells grown in roller bottles [23]. Purification by cesium chloride gradient of (ss)AAV8-hUGT1A1 resulted in two well-defined bands, corresponding to empty and full particles. Conversely, the full particle band obtained for (sc)AAV-hUGT1A1 was less intense and diffused (Figure 1B). This was associated with more than three-fold reduction in production yields (6.0±1.89 $x10^4$ vector genome (vg)/cell vs. 1.77±1.37 $x10^4$ vg/cell for (ss) and (sc)AAV, respectively, data obtained from at least two independent production lots). We then evaluated the analytical ultracentrifugation (AUC) profile of the full particles obtained for the two vectors. AUC performed on purified (ss)AAV8-UGT1A1 vectors, revealed, a sharp, single peak, with a sedimentation coefficient consistent with the size of the single stranded genome (Figure 1C). Conversely, for (sc)AAV8-hUGT1A1 vectors we observed the presence of different peaks, possibly due to the presence of AAV vectors containing DNA fragments of variable length (Figure 1D). The integrity of the genome was further analyzed by separation of purified vector genomes by electrophoresis under alkaline condition (Figure 1E), confirming the presence of a smear of vector genomes of different sizes in (sc)AAV8-hUGT1A1 vector preparations. Together, these data indicate that research grade (ss)AAV8-hUGT1A1 vectors were produced with higher yields and were more homogeneous than their self-complementary counterpart.

(ss) and (sc) AAV8-UGT1A1 vectors present equal potency profile in vitro and in vivo

We next compared the transduction efficiency of (sc)AAV8-hUGT1A1 vs. (ss)AAV8-hUGT1A1 *in vitro* in human hepatoma cells [19], which resulted in a similar expression of the

hUGT1A1 transgene (Figure 2A). Next, *in vivo* comparison of the vectors was performed in a well-established model of CN syndrome, the Gunn rat [25-27]. This model presents blood levels of bilirubin comparable to those observed in patients with mild symptoms and no evident signs of brain toxicity (6-12 ± mg/dL). (sc)AAV8-hUGT1A1 and (ss)AAV8-hUGT1A1 vectors titered side-by-side were injected intravenously in 8-week-old Gunn rats (n=10/group). Total bilirubin (TB) was measured in blood for about 7 weeks post-injection. Systemic injection of $1x10^{12}$ vg/rat [corresponding to $5.0x10^{12}$ vg/kg] of both vectors resulted in a complete and sustained normalization of circulating bilirubin levels (Figure 2B). Vector genome copy number (VGCN) analysis and hUGT1A1 protein expression levels in liver measured in treated animals confirmed the equivalence in potency of the two vectors (Figure 2C,D). A similar potency of (ss) vs. (sc) AAV8-hUGT1A1 vectors was also observed at $1x10^{10}$ and $1x10^{11}$ vg/rat (data not shown). In a separate experiment, Gunn rats were injected with $5x10^{11}$ vg/kg of (ss)AAV8-hUGT1A1 or (sc)AAV8-hUGT1A1. Three months after vector injection, bilirubin-glucuronide conjugates were present at similar levels in the bile of rats treated with the two vectors (Figure 2E). These data suggest that (ss) and (sc)AAV8-hUGT1A1 vectors used in the current study transduce hepatocytes equally both *in vitro* and *in vivo*. Based on the comparable efficacy of the two vectors, and the higher production yields and homogeneity profile, the (ss)AAV8-hUGT1A1 vector was selected as lead candidate for clinical development.

(ss)AAV8-hUGT1A1 can be efficiently produced in HEK293 cells grown in suspension.

A fully scalable method based on triple transfection of HEK293 cells cultured in suspension was developed to support the clinical development of (ss)AAV8-hUGT1A1 (Figure S1). Triple transfection of HEK293 cells was performed with polyethylenimine (PEI) directly in 10-liter bioreactors. AAV vectors were recovered from both supernatant and cells by mild detergent lysis followed by AVB Sepharose affinity column purification. Purified vectors were then concentrated and tested for quality and potency. (AUC) performed on (ss)AAV8-hUGT1A1 vector produced in suspension revealed that the product contained around 20% of full

capsids (data not shown). To better characterize the full to empty particles ratio, the purified (ss)AAV8-hUGT1A1 final product was loaded on a cesium chloride gradient and 16 fractions were collected and analyzed for capsid protein and DNA content. SDS-PAGE followed by Sypro® Ruby staining revealed the presence of the three bands corresponding to VP1, VP2 and VP3 at a ratio of 1:1:10 (Figure 3A). Two populations of particles, peaking at fraction 8 and 12-13 were identified. Subsequent quantitative PCR (qPCR) analysis showed that fraction 8 and 12-13 corresponded to full and empty particles, respectively (Figure 3B). Consistent with the AUC analysis, AAV particles present in fraction 8 represented 21% of the total VP protein, and qPCR data indicated that this fraction contained full capsids, representing 72.9% of AAV genomes present in all fractions.

We then evaluated the *in vitro* potency of the vector produced in suspension. Huh-7 cells were transduced with increasing multiplicity of infections (MOIs) of (ss)AAV8-hUGT1A1 produced in adherent cells or in suspension at 10L scale. Similar levels of hUGT1A1 protein were detectable by Western blot in cell lysates obtained from cells transduced with the two vector preparations (Figure 3C).

The equivalence of the two vectors was further confirmed *in vivo* in a juvenile Ugt1 knock-out mouse model ($Ugt1^{-/-}$) [16, 17]. These mice present a phenotype that closely resembles the human condition, therefore they need to be exposed to phototherapy (PT) to survive. Eleven-day-old mice were injected with $3.3x10^{9}$ vg/mouse (corresponding to $5.0x10^{11}$ vg/kg) of (ss)AAV8-hUGT1A1 vector produced in adherent or in suspension HEK293 cells. One-month post injection plasma bilirubin levels were determined and a complete correction of total serum bilirubin levels (about 1.0 mg/dl) was observed in mice treated with both AAV vector preparations (Figure 3D). VGCN analysis demonstrated that the two vectors transduced hepatocytes with similar efficacy (Figure 3E). Accordingly, expression of hUGT1A1 mRNA and protein levels in the livers of AAV vectors-treated $Ugt1^{-/-}$ mice analyzed 30 days post-treatment was comparable (Figure 3F,G). These results demonstrate that potency of vectors produced in bioreactors are fully comparable with research grade vectors derived from adherent cells.

Dose-finding studies with large-scale preparation of (ss)AAV8-hUGT1A1

We next scaled-up the 10-liter suspension AAV production to 200 liters. Several 200-liter lots of (ss)AAV8-hUGT1A1 vectors were produced, demonstrating robustness and reproducibility of the process. AUC analysis revealed that the large-scale product contained >30% of full capsids (Figure 4A). The vector potency was then evaluated *in vitro*. Treatment of Huh-7 cells at a 25,000 MOI of (ss)AAV8-hUGT1A1 resulted in hUGT1A1 protein levels similar to those obtained with adherent cells and medium scale (Figure S2). Next, a dose escalation study was conducted in Gunn rats, starting at vector doses that have previously shown therapeutic efficacy [19]. Two weeks after systemic injection of 6-8 week-old rats, blood samples were collected, and total bilirubin was analyzed. A dose-dependent decrease in levels of plasma TB was seen in animals treated with the (ss)AAV8-hUGT1A1 (Figure 4B). At a dose of $1x10^{12}$ vg/kg, 4/11 rats showed correction of TB levels, while at $2x10^{12}$ vg/kg in 8/10 rats a full correction of hyperbilirubinemia was observed (Figure 4B, and data not shown). Vector genome copies determined in whole livers of treated Gunn rats 84 days after treatment also showed a dose-dependent increase and correlated with the levels of correction of TB in serum. (Figure 4C). Based on these results, VGCN below 0.1 copies/cell were not sufficient to correct TB levels, as 13/14 animals with VGCN < 0.1 copies/cell had TB levels > 5 mg/dL. VGCN/cell in the range of 0.1 to 0.6 mediated TB correction in 6/14 rats, while all animals with VGCN/cell greater than 0.6 had normal TB levels.

Dose finding studies were also performed in $Ugt1^{-/-}$ mice. Adult (60-90 days old) male and female $Ugt1^{-/-}$ mice were injected with different doses of (ss)AAV8-hUGT1A1 (from $1.0x10^{11}$ to $5.0x10^{12}$ vg/kg) (Figure 5). Plasma bilirubin levels were monitored for 9 months post-injection. Male mice showed bilirubin levels below 0.5 mg/dl at all the doses tested, starting at $1x10^{11}$ vg/kg (Figure 5A). In female animals, in contrast, after the initial drop of TB levels to WT levels one month post-injection (Figure 5B), some animals lost expression over time (see

Figure S3 for single animal TB levels). Nine months post-injection mice were sacrificed, and livers were harvested for molecular analysis. Vector genome copy number (VG/cell) in whole livers showed a dose-response course (Figure 5C) and well correlated with the level of Ugt1a1 protein determined by Western blot analysis and immunofluorescence (Figure 5D and Figure S4). Some inconsistencies in vector dose response were noted in female animals, likely due to sex-specific differences in the efficiency of liver transduction in rodents [28]. Histological analysis of livers revealed no obvious abnormalities, as determined by H&E, Masson trichromic, Sirius red, PAS and Oil red-stainings (Figure S5).

We next performed an additional comparison study in mice and rats using an AAV8 expressing human coagulation factor IX (hFIX) under the transcriptional control of a liver specific promoter. We first ran a pilot study which demonstrated that the extent of liver transduction of AAV vectors in rats of Wistar and Sprague Dawley background is similar (data not shown). Then, we compared hFIX expression levels in Wistar rats (both wild-type and *Ugt1a1*$^{-/-}$) with C57Bl/6 mice. At a dose of $5x10^{12}$ vg/kg, mice showed levels of hFIX >10 µg/mL (Figure 5F), while rats expressed approximately 1.5µg/mL of hFIX. Interestingly, hFIX expression levels in rats were in a similar range, although still higher, of those observed in hemophilia B patients receiving $2x10^{12}$ vg/kg of a similar vector [12]. The evaluation of the vector genome copy number in the two species supported the findings on hFIX transgene expression levels (Figure 5G). Together, these results indicate that the rat is a good predictive model of the efficacy of liver gene transfer in humans, in particular for AAV8 vectors, and support further preclinical studies including toxicology/biodistribution study in this species.

GLP toxicity, biodistribution and shedding study to support the safety of liver gene transfer with (ss)AAV8-UGT1A1.

A GLP toxicology/biodistribution study was performed in wild-type adult Sprague Dawley rats. This was based on the observation that Wistar and Sprague Dawley have similar levels of liver transduction with AAV vectors (data not shown). The aim of this study was to

evaluate the potential toxicity, to determine shedding and biodistribution of the vector genomes after single intravenous administration of (ss)AAV8-hUGT1A1 in wild-type rats with a 26 weeks follow-up. Two vector doses were injected, one equivalent to the maximum planned clinical dose ($5x10^{12}$ vg/kg) and one five times higher ($2.5x10^{13}$ vg/kg).

Overall, the vector was well tolerated with no evident signs of toxicity. There were no unexpected deaths related to the treatment, no adverse in-life findings, no clinical pathology, no changes in biochemical and hematological parameters (Table 1), and no macroscopic findings in animals that received (ss)AAV8-hUGT1A1 and in control animals. Following i.v. administration, the vector was cleared from blood and urine within 29 days with levels of vector genomes completely undistinguishable from the limit of quantification (LOQ) of the measurement method (Figure 6A, B). Eight days after vector injection, VGCN and hUGT1A1 mRNA expression levels were measured. No differences in biodistribution were observed between male and female rats. The highest copies of vector were detected in the liver, spleen and lymph nodes, reflecting the tropism of AAV8 vector following i.v. delivery. hUGT1A1 mRNA was detectable on day 8 in all tissues, at levels at least 2-log lower than those measured in the liver, which was the tissue with the highest copies and the highest mRNA expression, reflecting the specificity of the promoter expressing the hUGT1A1 transgene (Figure 6C and Table S1). Expression of hUGT1A1 in the liver at day 91 and 182 did not show any significant decrease in transgene expression (Figure 6D). Transgene expression was further confirmed by *in situ* hybridization (ISH) in rat liver tissue at day 182 (Figure 6E), showing ~11.5% of hepatocytes expressing the UGT1A1 transgene.

Persistence of vector in gonads at low levels (VGCN <0.1 per diploid genome) was detected 6 months post-treatment. Based on this, although the risk of germline transmission is expected to be low, we used ISH to further investigate the exact localization of the vector within the gonads. While a signal was localized in ovaries of rats injected with the highest vector dose, positivity was detectable only within the stroma and in blood capillaries. No signal was detected in oocytes (Figure 6F).

A separate GLP study was aimed at assessing the risk of germline transmission in male animals. (ss)AAV8-hUGT1A1 was administered to male rabbits at a dose of $5x10^{12}$ vg/kg. Vector genomes were determined by qPCR in liver, testis and epididymis, collected at day of sacrifice, 150 days after treatment (Figure 6G). Vector shedding in sperm was evaluated pretreatment and at day 3, 7, 15, 30, 60, 90, 120 and 150 post-treatment. Genomes were quantifiable from Day 3 to Day 30 and became completely undetectable thereafter (Figure 6H).

These results indicate that the single intravenous injection of (ss)AAV8-hUGT1A1 vector was well tolerated at doses up to $2.5x10^{13}$ vg/kg. They also indicate that the risk for germline transmission at the doses tested is likely to be very low.

In mice and rats, (ss)AAV8-hUGT1A1 drives the development of humoral responses directed to the human transgene

Humoral immune responses against AAV8 and hUGT1A1 were measured in the context of the GLP toxicology study in rats. All animals developed a significant humoral immune response against the AAV8 capsid starting at day 8 and regardless of the dose infused (Table 2). Some animals also developed binding IgG against the human UGT1A1 protein (Table 2). To understand the origin of this response, we measured the formation of anti-transgene antibodies in $Ugt1^{-/-}$ deficient mice treated with AAV8 vector carrying the mouse UGT1A1 transgene (mUGT1A1). Total bilirubin in plasma, transgene expression and humoral response directed against the transgene were assessed. Long-term correction of TB was observed in both male and female animals (Figure 7A), along with vector genome persistence (Figure S6A) and UGT1A1 protein expression in liver of treated animals (Figure 7B, Figure S6B). No anti-mUGT1A1 binding antibodies were detected in plasma of treated mice one month post injection, while 3 out of 4 of the mice dosed with the human construct (hUGT1A1) had detectable antibodies (Table 3).

Similar results were obtained in Gunn rats. AAV8-UGT1A1 vectors encoding for both human and rat transgene corrected plasma TB (Figure 7C). VGCN analysis demonstrated that the

two vectors transduced hepatocytes (Figure S6C) and similar expression of the UGT1A1 protein was observed (Figure S6D). Anti-human UGT1A1 binding antibodies were measured by ELISA (Figure 7D) and anti-rat UGT1A1 binding antibodies were measured by Western blot (Figure 7E). Also in this case, the species-specific version of the UGT1A1 transgene appeared to be less immunogenic than the human counterpart (Table 3).

These results indicate that the human UGT1A1 transgene elicits humoral responses in rodents, supporting the use of species-specific transgenes to more carefully assess transgene immunogenicity.

Administration of glucocorticoids in conjunction with (ss)AAV8 hUGT1A1 gene transfer is safe in mouse and rat models of Crigler-Najjar syndrome.

Immune response triggered by AAV is a potential concern for gene therapy clinical applications, and based on the experience with AAV8-mediated liver gene transfer for hemophilia B, it is known that a short course of corticosteroids may be needed to control the immune response directed against the vector [11, 12].

To identify possible interactions of corticosteroids with AAV gene transfer in CN animals, we used both Gunn rats and Ugt1$^{-/-}$ mice. In Gunn rats, a tapering course of corticosteroid was given 4 weeks post gene transfer. No detrimental effect on correction of TB levels was observed (Figure 8A). Accordingly, no effect of methylprednisolone treatment on VGCN was noted (Figure 8B), and no obvious treatment-related effects on transaminases activities were measured (Figure S7A). Similar experiments were performed in adult Ugt1$^{-/-}$ mice, treated daily with methylprednisolone starting one day before vector administration (Figure 8C). No adverse effects were noted following methylprednisolone treatment, as correction of TB levels with (ss)AAV8-hUGT1A1 was achieved in mice with or without corticosteroids (Figure 8D). Accordingly, liver enzymes in methylprednisolone-treated and control mice remained unchanged (Figure S7B). Histological analysis of the liver 9 months post injection showed no major abnormalities in mice treated with corticosteroids compared to their controls (Figure

S7C-G). Finally, molecular analysis of VGCN showed no significant effect of corticosteroid on liver transduction (Figure 8E, p=0.1608, sham vs. MePRDL).

These results demonstrate the safety of glucocorticoids administration concomitant to gene transfer in animal models of CN syndrome.

DISCUSSION

Gene therapy with AAV vectors holds the potential for a curative treatment for several liver metabolic disorders [10]. Among them, Crigler-Najjar syndrome appears to be an ideal candidate [8].

Here we propose the use of a single stranded AAV8 vector driving the liver-specific expression of hUGT1A1 for the safe and efficient correction of hyperbilirubinemia, the pathological hallmark of CN syndrome.

In order to select the best candidate for clinical development, we compared a (sc)AAV8 vector designed for the expression of hUGT1A1 with an optimized (ss)AAV8 vector [21]. (sc)AAV and (ss)AAV vectors have been used to transduce the liver in the context of several genetic disorders [10]. To this aim, the use of (sc)AAV vectors could provide potential advantages related to the bypass of the step of dsDNA conversion of the vector genome, thus facilitating the viral transduction [29]. However, the use of (sc)AAV vectors has potential drawbacks, including the reduced genome packaging capacity, the lower vector production yields, and the low homogeneity at least in the context of the current study) due to the production of vectors containing truncated genomes. Hence, here we carefully characterized (sc)AAV8-hUGT1A1 and (ss)AAV8-hUGT1A1 vectors and we showed that, using research-grade production method, (ss)AAV8-hUGT1A1 vectors were generated with higher yields and superior product homogeneity.

Several studies have been published in which both (sc) and (ss) AAV vectors were used to transduce the human liver, these include trials for hemophilia B [12, 13, 30], hemophilia A [14], and acute intermittent porphyria [31]. In the present work, we demonstrated in the Gunn rat model of CN, that the clinical candidate (ss)AAV8-hUGT1A1 vector has a similar potency than a (sc)AAV vector carrying the same transgene, both in term of therapeutic efficacy and liver transduction level. One caveat of the current work is that, due to the size of the UGT1A1 transgene and the reduced genome packaging capacity of self-complementary AAVs (~2.5 Kb), the expression cassettes of the (ss) and (sc) AAV8-hUGT1A1 vectors were not identical.

Future studies with vectors carrying exactly the same expression cassettes will help to more carefully compare the potency of vectors carrying different genome configurations.

Considerations over the ability to produce (sc)AAV vectors in sufficient quantity and of acceptable quality, and concerns over the potential higher immunogenicity of these vectors [32], prompted us to focus on a (ss)AAV8-hUGT1A1 vector to develop a scalable production process specific for this vector construct. A scalable animal product-free GMP manufacturing-compliant process for (ss)AAV8-hUGT1A1 vectors production was developed. The process consisted of transient tri-transfection of HEK293 cells cultured in suspension in bioreactors [33], which was able to supply vector in sufficient quantities to support preclinical and clinical development of the investigational gene therapy candidate. One difference between the suspension manufacturing method and the research-grade production system used in this study resides in the downstream process, which in the suspension process consists of a scalable column-based affinity purification technique, no longer efficient in eliminating the empty particles in the final product. As already highlighted [34], the consequences of the presence of empty capsids in the final product remain unclear, although preparations of AAV vectors containing both capsid species have been safely used in several liver gene transfer clinical trials [11-15]. Additionally, it has been shown that the optimization of the ratio of full to empty capsids in the final formulation of the therapeutic vector could maximize the efficacy of gene transfer [35], as the empty capsid can act as decoys for anti-AAV neutralizing antibodies. Here, we compared the potency of (ss)AAV8-hUGT1A1 vectors generated with two production methods, one leading to full AAV particles only and the other leading to a mix of empty and full capsids. We demonstrated a similar potency of the two vector preparations both *in vitro* and *in vivo*. We showed that the (ss)AAV8-UGT1A1 vectors produced in suspension and containing empty particles efficiently correct hyperbilirubinemia in CN mice and reached similar liver transduction levels when compared to research-grade vector preparations composed by full particles only.

One important aspect of the current study is that it validates the rat as an ideal model of liver gene transfer. Through a careful comparison of the AAV vector liver transduction efficiency in

rats and mice, we provided evidence that the efficiency of liver transduction of AAV8 vectors in rats is similar to that expected in humans. Conversely, AAV8 vectors transduce the mouse liver with at least a log higher efficiency, thus potentially overstating the therapeutic efficacy of a gene therapy drug candidate. Accordingly, using a (ss)AAV8-hFIX vector, we observed lower liver transduction in Gunn rats than in mice. At the same vector dose ($5x10^{12}$ vg/kg) hFIX transgene expression levels detected in blood of mice were ~100% of those measured in humans. Conversely, the injection of the same vector dose in rats resulted in levels of hFIX in the same range of those described in humans receiving a comparable vector dose ($2x10^{12}$ vg/kg) of a similar AAV8 vector encoding for hFIX [11, 12]. These data support the concept that, when available, rats are animal models suitable for dose-finding studies, in particular for AAV8 vectors, and their use in the current study provided a valuable tool to support the choice of a starting dose of vector to be used in the clinic, which holds the prospective of driving therapeutic efficacy in humans.

Efforts were then focused on the manufacturing process scale-up. (ss)AAV8-hUGT1A1 vectors were produced at a 200-liter scale. Vector preparations were carefully analyzed for both the content of full and empty capsids and DNA contaminants, among others. Notably, for the determination of empty to full capsid ratio, here we used AUC, a method that has been demonstrated to provide a reliable readout [36, 37].

GLP-compliant biodistribution studies confirmed the expected tissue distribution of AAV8 vectors. However, due to the low-level persistence of vector genomes in gonads 6 months post vector infusion, a germline transmission study was performed in male rabbits. As already reported in animal models and humans [11, 12, 38], vector was transiently detected in the sperm of rabbits indicating a negligible risk of germline transmission that could be further mitigated by physical barrier contraception during the clinical trial. Similarly, ISH studies in female rats confirmed that AAV vectors do not transduce efficiently oocytes, as previously shown using a reporter vector [39].

In our GLP toxicology and biodistribution study, all animals developed a significant humoral immune response against the AAV8 capsid, a result that is largely expected [40]. Some animals also developed IgG against the hUGT1A1 protein. Development of anti-human UGT1A1 antibodies has been also documented following the administration of AAV-hUGT1A1 [18], in studies conducted in CN rats, with no consequence on the vector efficacy [21]. The development of anti-hUGT1A1 antibodies is not considered as toxicologically relevant as no elevations of transaminases or treatment-related histopathological findings were noted in the GLP toxicity study. Nevertheless, we further investigated the origin of this finding by testing whether the immune response was driven by the human transgene expressed in rats. To this aim, we injected rat and mouse UGT1A1 transgenes in the corresponding rat and mouse models of CN syndrome. The absence of humoral response directed against rat UGT1A1 in Gunn rats and mouse UGTA1 in the $Ugt1^{-/-}$ mouse model suggests that the anti-hUGT1A1 antibodies observed in the GLP study in rats originated from species-specific transgene immunogenicity. One important implication of this work is that it indicates that immune responses observed in animal models may be driven by species-specific reactions to the transgene expressed, which in some cases may confound the readout of preclinical studies.

Finally, as glucocorticoids have been used to modulate vector immunogenicity in several trials [11-15, 41], here we tested the safety of the approach in the context of CN syndrome. Immunosuppression can indeed affect the safety and efficacy of gene transfer [42, 43]; here we demonstrated in two animal model of CN syndrome that methylprednisolone administration had no impact on the safety and efficacy of the gene therapy.

In conclusion, this work describes the development of an investigational gene therapy for CN syndrome based on an AAV8 vector injected intravenously to deliver a corrected copy of the UGT1A1 gene to hepatocytes. The vector construct has been optimized for liver-restricted expression and is based on a gene delivery platform with proven excellent safety and

efficacy profile in humans. We showed successful and efficient manufacturing scale-up and described a comprehensive approach to safety and efficacy in preclinical studies. This work constitutes the basis for the initiation of an AAV-mediated gene therapy clinical trial in CN.

MATERIALS AND METHODS

Plasmids construct

The transgene expression cassette of the (ss)AAV8-hUGT1A1 carrying a codon-optimized cDNA sequence encoding for human UGT1A1 was previously described [21]. This construct (also known as GNT0003) was selected as the clinical candidate (NCT03466463). The cassette contains the human hemoglobin beta (HBB)-derived synthetic intron (HBB2) [44] and the HBB polyadenylation signal. The transgene expression cassette of the (sc)AAV8-hUGT1A1 was developed by Dr Bosma (Academic Medical Center, Amsterdam, Netherlands) and consisted of a codon-optimized cDNA sequence encoding for human UGT1A1 transgene cloned into a (sc)AAV backbone. This plasmid carries the AAV2 inverted terminal repeats (ITR)s with an intact 5' terminal resolution site (trs) without the analogous 3' trs, a hybrid liver-specific promoter (HLP), a modified SV40 small intron [45] sequence and the SV40 late polyadenylation signal. For the in vitro comparison of hUGT1A1 expression levels, we used a (ss)AAV8-GFP as a control. The expression cassette contained the cDNA sequence encoding for enhanced green florescent protein (eGFP) transgene, the phosphoglycerate kinase (PGK) promoter, and a SV40 polyA sequence. For the in vivo comparative study between mice and rats, we used a (ss)AAV8 vector expressing coagulation factor IX under the transcriptional control of a liver specific promoter [46].

Production of AAV vectors

Research-grade AAV vectors used in this study were produced using a slight modification of the adenovirus-free transient transfection methods described . Briefly, adherent HEK293 cells grown in roller bottles were transfected with the three plasmids containing the adenovirus helper proteins, the AAV Rep and Cap genes, and the ITR-flanked transgene expression cassette. 72 hours after transfection, cells were harvested, lysed by sonication, and treated with Benzonase® (Merck-Millipore, Darmstadt, Germany). Vectors were then purified using two successive ultracentrifugation rounds in cesium chloride density gradients. Full capsids were collected, the final product was formulated in sterile phosphate buffered

saline containing 0.001% of Pluronic (Sigma Aldrich, Saint Louis, MO), and stored at -80 °C. GMP-like (ss)AAV8-hUGT1A1 vectors used in this study were produced in bioreactor and at different scales up to 200 liters by adenovirus-free transient transfection method. Suspension HEK293 cells were transfected with Polyethyleneimine (PEI) (PEIpro, Polyplus) with the three same plasmids mentioned above. Twenty-four hours after transfection, cells were treated with Benzonase® and two days later, they were lysed with Triton ((Sigma, St Louis, MO) and clarified by filtration. Vectors were purified by a single chromatography column based on AVB Sepharose immuno-affinity (GE Healthcare) before concentration by tangential flow filtration. Purified particles were formulated in Ringer-Lactate solution containing 0.001% Pluronic (F68), vialed and stored at −80 °C.

Characterization of AAV vectors

Titers of AAV vector stocks were determined using quantitative real-time PCR (qPCR). Specific probe and primers were as follows: forward 5'-GGCGGGCGACTCAGATC-3', reverse 5'-GGGAGGCTGCTGGTGAATATT-3', probe 5'-AGCCCCTGTTTGCTCCTCCGATAACTG-3'.

To perform alkaline agarose gel, viral DNA were extracted from 100µL of AAV solutions. Samples were denatured 5 minutes at 95°C and prepared in 6X alkaline loading buffer (300mM NaOH, 6mM EDTA, 18% Ficoll, 0.5% bromocresol green, 0.25% xylene cyanol) and GelRed1X. After electrophoresis in denaturing conditions (50mM NaOH-1mM EDTA), gel was stained with GelRed diluted 1:10 000.

Analytical Ultra Centrifugation measures the sedimentation coefficient of macromolecules by following over time the optical density of a sample subjected to ultracentrifugation. The difference in the sedimentation coefficient, measured by Raleigh interference or 260 nm absorbance, depends on the content of viral genome in the capsid. AUC analysis was performed using a Proteome Lab XL-I (Beckman Coulter, Indianapolis, IN). 400µL of AAV vector and 400µL of formulation buffer were loaded into a two-sector velocity cell. Sedimentation velocity centrifugation was performed at 20,000 rpm and 20°C. Absorbance

(260 nm) and Raleigh interference optics were used to simultaneously record the radial concentration as a function of time until the lightest sedimenting component cleared the optical window (approximately one hour and a half). Absorbance data required the use of extinction coefficients to calculate the molar concentration and the percent value of the empty and genome-containing capsids. Molar concentrations of both genome-containing and empty capsid were calculated using Beer's law and % full genome-containing and empty capsid was calculated.

For the characterization of the VP proteins content in the different populations of particles, AAV8-hUGT1A1 vectors were loaded in cesium chloride solution (1.38g/cm^3) and ultra-centrifuged at 38000rpm and 20°C for 40h. The total volume of the viral/cesium solution was then collected in 16 fractions (0.5mL). The CsCl was removed from the fractions by repeated dialysis cycles against PBS-0.001% pluronic F68 solution. A volume of 10µL of each fraction were loaded onto a 4-12% SDS-polyacrylamide gel (Thermo Fisher Scientific, Waltham, MA). After protein migration, the gel was stained with a SYPRO® Ruby solution (Invitrogen, Carlsbad, CA).

hUGT1A1 expression in Huh7 cell line

For transduction experiments, six-well plates containing 80% confluent Huh-7 cells were transduced with AAV8-UGT1A1 vectors at the indicated MOI. AAV8-GFP transduced cells were included as control. 72 hours after transduction cells were harvested and frozen at -20°C until processing. Microsomes extraction was performed at 4°C. Frozen cell pellets were resuspended in 300µL of lysis buffer (20mM Hepes, 1% Triton X-100), proteases inhibitor cocktail (Sigma Aldrich, Saint Louis, MO) and centrifuged 5 minutes at 100xg. Supernatants were collected and centrifuged 60 minutes at 18000 g. Pellets were resuspended in 100µL of 20mM Hepes and the protein concentration was determined using the BCA Protein Assay kit (Thermo Fisher Scientific, Waltham, MA), following the manufacturer's instructions. Microsomal extracts were separated on a 4-12% bis-tris polyacrylamide gel (Thermo Fisher Scientific, Waltham, MA). The same amount of protein was loaded in each lane. The gel was

transferred onto a nitrocellulose membrane and blotted with an anti-UGT1A1 antibody (SantaCruz biotechnology, Santa Cruz, CA) and an anti-actin antibody (Sigma Aldrich, Saint Louis, MO), used as loading control. Secondary antibodies and detection system were from Li-Cor Biosciences (Lincoln, NE).

Animal experiments

Ugt1$^{-/-}$ mice have been described previously [16]. Wild type or Ugt1$^{-/-}$ untreated littermates were used as controls as indicated. Mice were housed and handled according to institutional guidelines, and experimental procedures approved by the International Centre for Genetic Engineering and Biotechnology board. Animals used in this study were at least 99.8 % C57BL/6 genetic background, obtained after more than 9 backcrosses with wild type C57BL/6 mice. Mice were kept in a temperature-controlled environment with 12/12 hour light–dark cycle. They received a standard chow diet and water ad libitum.

The Gunn rat is a natural occurring model of CN syndrome that has no residual UGT1A1 enzyme activity. Rats and wild-type C57BL/6 mice used in this study were fed ad libitum and were housed and handled according to institutional guidelines. All in vivo experimental procedures were approved by the French, and Italian competent authorities and Ethical Committees (ref. 2013007C and 2017002B_APAFIS#9667) according to the European Directive 2010/63/EU.

Both male and female animals were used, to better represent the CN patient population which includes both male and female individuals.

Gene transfer procedures and phototherapy treatment

Ugt1$^{-/-}$ mice: Post-natal day 11 (P11) mice were intraperitoneally injected with AAV vectors or saline. Newborns were exposed to blue fluorescent light (Philips, Amsterdam, The Netherlands) for 12 hours per day (synchronized with the light period of the light/dark cycle) up to 12 days after birth and then maintained under normal light conditions. Intensity of the blue lamps was monitored monthly with an Olympic Mark II Bili-Meter (Olympic Medical, Port

Angeles, WA). For adult studies, Ugt1$^{-/-}$ animals were exposed to blue fluorescent lamps up to day 20 after birth as previously described [20]. Blood samples were collected at sacrifice by facial vein exsanguination. Liver tissues were collected at sacrifice for transgene expression assessment. For immunogenicity study and glucocorticoids administration evaluation, PBS or AAV vectors were administrated in adult (P60-P90) Ugt1$^{-/-}$ mice by intravenous injection in retro-orbital sinus. Blood samples and liver tissues were collected at sacrifice for transgene expression assessment.

Gunn rats: 6-8 weeks old rats were injected intravenously via the tail vein with AAV vectors or saline. Blood samples were collected by retro-orbital venipuncture every week after AAV injection. To determine transgene expression, liver tissues were collected at sacrifice. For analysis of bilirubin glucuronides, bile samples were collected in this experiment at 3 months post injection.

C57BL6 mice: 6-8 weeks old mice were injected intravenously via the tail vein with AAV vectors or saline. Blood samples were collected by retro-orbital venipuncture and liver tissues were collected at sacrifice.

Bilirubin measurement

Total Bilirubin determination in mice and rats was performed in plasma as previously described. Plates were read at 560 nm on an Enspire plate reader (Perkin Elmer, Waltham, MA). Bilirubin conjugates in bile were analyzed and quantified by HPLC as previously described [18] using an Omnisphere column (Varian, Palo Alto, CA) for the separation of bilirubin conjugates [47].

hFIX measurement

Levels of hFIX in plasma were quantified with an enzyme-linked immunosorbent assay (ELISA) as described [46]. Capture antibody (PierceTM Factor IX Antibody - MA1-43012) was used at 2.8µg/mL, left overnight at 4°C, washed with PBS containing 0.05% Tween 20 (PBST), and blocked with 200µL/well of blocking buffer (6% milk in PBST) for 2 hours at

37°C. Standards were prepared by serial dilutions of purified recombinant hFIX (starting concentration, 1000µg/mL). A horseradish peroxidase (HRP)–conjugated goat polyclonal anti-hFIX Ab (Affinity Biologicals, Ancaster, ON, Canada) diluted 1:1000 was used as secondary antibody.

Clinical Biochemistry

After prednisolone administration, activities of ALT and AST in rat plasma were measured on days 28, 35, 42 and 70 using colorimetric ALT and AST activity assay kits (Sigma, St Louis, MO). Plates were read on an Enspire® plate reader (Perkin Elmer, Waltham, MA).

Virus vector genome copy number analysis

To reduce variability generated by uneven transduction of liver parenchyma by AAV vectors, whole rat livers were homogenized in 20mM Hepes, 250mM sucrose. For mouse samples, livers were harvested 1 month post-injection, pulverized in liquid nitrogen and aliquoted for further molecular analysis. The following primers and probes were used: UGT1A1 forward 5'-GGCGGGCGACTCAGATC-3', reverse 5'-GGGAGGCTGCTGGTGAATATT-3', probe 5'-AGCCCCTGTTTGCTCCTCCGATAACTG-3'; titin forward 5'-AGAGGTAGTATTGAAAACGAGCGG-3', reverse 5'-GCTAGCGCTCCCGCTGCTGAAGCTG-3', probe 5'-TGCAAGGAAGCTTCTCGTCTCAGTC-3'. VGCN in mice was quantified by qPCR using specific primers for the hAAT promoter as previously described [17].

Preparation of total RNA, RT-PCR and Real Time PCR analysis

Total RNA from mouse liver was prepared using EuroGOLD Trifast (Euroclone) according to manufacturer's instructions. 1 µg of total RNA was reverse-transcribed using M-MLV (Invitrogen, Carlsbad, CA) and oligodT primer according to manufacturer's instructions. Total cDNA (1µl) was used to perform either RT-PCR or qPCR using specific primers : forward 5'-TAAATACGGACGAGGACAGG-3', reverse 5'-ACCTCCTTGTGATTCCACAG-3'. qPCR was

performed using iQTM SYBR® Green Supermix (Bio-Rad, Hercules, CA) and a C1000 Thermal Cycler CFX96 Real Time System (Bio-Rad, Hercules, CA). Expression of the gene of interest was normalized to Gapdh house-keeping gene, using specific primers: forward 5'-ATGGTGAAGGTCGGTGTGAA-3', reverse 5'- GTTGATGGCAACAATCTCCA-3'. Real Time PCR data were analyzed using the ΔΔCt method.

Microsomes extraction and Western blot analysis

From 500µL of liver homogenate, microsomes extraction was performed at 4°C. Rat liver samples were centrifuged 5' at 100g, mixed with 4.5 mL of 20mM Hepes buffer and centrifuged at 10000g for 10 min. Supernatants were then centrifuged at 20000g for 60 min. Pellets were resuspended in 400µL of 20mM Hepes and the protein concentration was determined using the BCA Protein Assay kit (Thermo Fisher Scientific, Waltham, MA), following the manufacturer's instructions. Microsomal extracts were separated on a 4-12% bis-tris polyacrylamide gel (Thermo Fisher Scientific, Waltham, MA). The same amount of protein was loaded in each lane. The gel was transferred onto a nitrocellulose membrane and blotted with an anti UGT1 rabbit polyclonal antibody (SantaCruz Biotechnology, Santa Cruz, CA). Anti-actin (Sigma Aldrich, Saint Louis, MO), was used as loading control. Secondary antibodies and detection system were from LiCor Biosciences (Lincoln, NE).

For mouse samples, liver powder was homogenized in RIPA Buffer (150 mM NaCl, 1% NP-40, 0.5% DOC, 0.1% SDS, 50 mM Tris HCl pH8, 2x protease inhibitors) and analyzed by Western blot analysis as described previously [16].

GLP toxicity/biodistribution study

This study was performed in Charles River (Tranent, UK) and Genosafe (Evry, France) laboratories. Hundred 5-7 old wild-type Sprague Dawley rats were divided in 3 groups. Animals were treated either with (ss)AAV8-hUGT1A1 vector at $5x10^{12}$ vg/kg or at $2.5x10^{13}$ vg/kg or with PBS on day 0 by intravenous injection into the lateral tail vein. Follow up of 3

weeks, 3 months and 6 months were realized on the animals to evaluate the potential toxicity of the vector.

Clinical signs, body weight changes, food and water consumption, and clinical pathology parameters were evaluated during this study. For hematology, coagulation, clinical chemistry, urinalysis and immunogenicity assessment, blood and urines samples were collected in each group at different time points from day 6 to the day of sacrifice. Urines and blood samples were also collected for shedding analysis at days 2, 4, 6, 15 and 28 after injection. Gross necropsy findings, organ weights, biodistribution of the vector and histopathologic examinations were conducted in animals euthanized 8, 91 and 182 days after vector administration.

GLP germline transmission study

This study was performed in Centre de Recherche Biologiques (CERB) (Baugy, France) and Genosafe (Evry, France) laboratories. Adult New Zealand White male rabbits were used for this study. (ss)AAV8-hUGT1A1 vectors or vehicle were administered once on day 1 by the intravenous route as a slow bolus over about 1 minute in the marginal ear vein in a volume of 0.9 mL/kg. Morbidity/mortality checks were performed twice daily. Clinical observations were performed before dosing and daily during the study. Body weights were recorded on day 1, 3, 5, 7, 9, 15 and then once a week. Sperm samples were collected before dosing and on day 3, 7, 15, 30, 60, 90, 120 and 150. All animals were sacrificed on day 150. Selected organs (testis and epididymis, liver) were sampled on the day of necropsy then analyzed for biodistribution assessment.

GLP In Situ Hybridization (ISH)

This study was performed by Cytoxlab (Evreux, France). Briefly, the ISH method was automated and performed on Formalin-Fixed Paraffin-Embedded (FFPE) tissues. The sections were pre-treated by heating at +97°C for 24 minutes and subsequently incubated with a protease for another 16 minutes at 37°C. The probes of interest (Advanced Cell

Diagnostic Inc., Newark, CA) were then hybridized at +43°C for 2 hours. The amplification and detection systems were applied following the manufacturer recommendations (RNAscope® 2.5 VS, Advanced Cell Diagnostic Inc., Newark, CA). The sections were stained with hematoxylin for 8 minutes and subsequently bluing reagent for 4 minutes. The slides were thoroughly washed in soap water for 2 minutes followed by running water for additional 2 minutes. Finally, all slides were mounted.

Detection of Anti-AAV8 Antibodies in Rat Plasma

MaxiSorp 96-wells plates (Thermo Fisher Scientific, Waltham, MA) were coated with AAV8 capsids in carbonate buffer at 4°C overnight. A standard curve of rat IgG (Sigma Aldrich, Saint Louis, MO) prepared as seven 2-fold dilution steps starting at 1µg/mL was coated onto the wells. After blocking, plasma samples were added to plates and incubated 1 hour at 37°C. Secondary antibody was added into well (anti-Rat IgG-HRP) and plates were developed with 3,3′,5,5′-tetramethylbenzidine substrate and the optical density was assessed by spectrophotometry at 450 and 570 nm (for background subtraction) on Enspire plate reader (Perkin Elmer, Waltham, MA) after blocking the reaction with 5% H2SO4.

Detection of Anti-UGT1A1 Antibodies in Rat Plasma

Human UGT1A1. Same ELISA protocol as described above was followed, but using for this specific experiment, the UGT1A1 protein to coat the plates.

Rat UGT1A1. To detect antibodies against the rat UGT1A1 protein, 40µg of microsomal extracts from liver tissues expressing or not rat UGT1A1 transgene were separated on a 4-12% bis-tris polyacrylamide gel (Thermo Fisher Scientific, Waltham, MA) and blotted onto a nitrocellulose membrane. Serum of each rat was used to develop a separate membrane as primary antibody (1:100). As a positive control, serum from rats immunized with UGT1A1 (1:200) and commercial anti-UGT1 rabbit polyclonal antibody (Millipore, Burlington, MA) were used. A positive signal, corresponding to the rUGT1A1 band, is detected only when

antibodies against rUgt1a1 are present in the plasma of the animal. Secondary antibodies and detection system were from Li-Cor Biosciences (Lincoln, NE).

Detection of Anti-UGT1A1 Antibodies in Mouse Plasma

The determination of anti-human Ugt1a1 antibodies in mouse plasma has been described previously [19, 20], while the determination of anti-mouse UGT1A1 antibodies was performed with a minor modification of the previous protocol. HuH7 cell line was infected with an AAV8 containing the mouse WT UGT1A1 cDNA (25000 MOI) and 72 hours later cell were harvested and total cell protein extract was prepared. 20 µg of total protein extract derived from uninfected and AAV-infected cells were separated in a 10% sodium dodecacyl sulfate polyacrylamidegel electrophoresis, blotted onto nitrocellulose membrane. Plasma from individual animals was used as primary antibody (1:200).

Methylprednisolone treatment

Gunn rats. 6-8 week old rats were divided into four groups. Animals were treated either with i.v. (ss)AAV8-hUGT1A1 vector or PBS on day 0. Later the rats were treated i.p. daily with Methylprednisolone (Solu-Medrol) or PBS utilizing the following schedule: 5 mg/kg prednisolone for 7 days, 2.5 mg/kg for next 2 days, 1.3 mg/kg for next 2 days, 0.6 mg/kg for next 2 days and 0.2 mg/kg for last 2 days. The groups that received PBS on Day 0 were treated with prednisolone or PBS between days 21 and 35. The groups that received rAAV8-hUGT1A1 vector on day 0 were treated with prednisolone or PBS between days 28 and 42. Blood samples were collected during three months after AAV injection at several time points. Animals were sacrificed on day 84 and liver were collected.

Ugt1$^{-/-}$ *mice*. Adult mice (8-12 weeks old) were injected retro-orbitally with (ss)AAV8-hUGT1A1 at the dose of $1x10^{12}$ or $5x10^{12}$ vg/kg. One day before the vector treatment animals were treated i.p. with methylprednisolone (Solu-Medrol). Methylprednisolone was applied as five consecutive daily injections at the doses of 5.0, 2.5, 1.3, 0.6, 0.2 mg/kg/day. Animals were sacrificed on day 84 and blood and liver were collected.

Histological analysis of liver sections.

At sacrifice livers biopsies from AAV-treated animals and wild-type and Ugt1-/- untreated littermates were extracted and fixed with 4% paraformaldehyde (PFA) in PBS overnight at 4°C. The next day biopsies were immersed in 20% sucrose in PBS and 0.02% sodium azide and kept at 4°C.

For immunofluorescence analysis and Oil red staining after cryoprotection in specimens were frozen in optimal cutting temperature compound (BioOptica, Milano, Italy) and 14 µm slices were obtained in a cryostat. For Ugt1a1 immunofluorescence liver specimens (14 µm) were incubated in sodium citrate pH9 prior to blocking solution. Next, specimens where blocked in 10% normal goat serum (Dako) and then incubated with the primary antibody (1:200; Sigma, St. Louis, MO) for 2 hours at room temperature. Specimens were incubated with secondary antibody Alexa fluor 488, Invitrogen). Nuclei were visualized by adding Hoechst (10 µg/ml) and mounted with Mowiol 4-88 (Sigma). Oil red staining was performed according to manufacturer instructions (Bioptica, Milano, Italy). Periodic-acid staining (Sigma, St. Louis, MO) was performed according to manufacturer instructions. Sirius red staining, sections were de-waxed and hydrated; nuclei were stained with Weigert hematoxylin, washed in tap water and then incubated with picro-sirius red for 1 hour (Sigma, St. Louis, MO). After two washes in acidified water sections were dehydrated in absolute ethanol, cleared in xylene and mounted in Eukitt (Sigma, St. Louis, MO). Images were acquired on a Nikon Eclipse18 E-800 epi-fluorescent microscope with a charge-coupled device camera (DMX 1200F; Nikon,19 Amstelveen, The Netherlands). Digital images were collected using ACT-1 (Nikon) software.

Statistical analyses

Results are expressed as mean ± SEM or mean ± SD as described in the text. The Prism package (Graph Pad Software, La Jolla, CA) or StatistiXL plugin for windows Excel were used to analyze data and prepare the graphs. Statistical analyses have been performed by

one way or two-way ANOVA as described in the text. Values of $p < 0.05$ were considered as statistically significant.

CONFLICT OF INTEREST STATEMENT

F.C., G.B., G.R., P.J.B., A.F.M., F.M., are inventors in patents describing the AAV technology and gene therapy-based treatments for Crigler-Najjar syndrome. All other authors declare no conflict of interests with the work presented here.

ACKNOWLEDGMENTS

This work was supported by the European Union's H2020 research and innovation program under Grant Agreements No. 755225 (CureCN, coordinated by F.M.). It was also supported by Genethon, the Association Française contre les Myopathies (AFM), a grant from CIAMI Association of Crigler-Najjar Patients Italy (to F.M.), the ASTRE grant from Conseil Départemental de l'Essonne (to F.M.), a ZonMW TGO grant (to P.J.B.), the Najjar fund (to P.J.B.), the Beneficentia Stiftung (to A.F.M.), and the EU Marie Slodowska-Curie fellowship agreement number 658712-3 (to G.R.).

AUTHORS CONTRIBUTIONS

C.L.B., P.J.B., A.F.M., G.R., M.H., and F.M. contributed to the experimental design, supervised experiments and results interpretation, and wrote the manuscript. F.C., G.B and L.G. contributed to experimental design, performed experiments and analyzed the data, contributed to results interpretation and manuscript preparation. T.B. contributed to the GLP studies management. S.C. and L.v.W. contributed to the in vivo experiments. S.J.A., Pa.V., P.V., M.S.S., S.R., D.G.D., F.L., C.L., and S.M. contributed to the experimental activities.

REFERENCES

1. Crigler, J.F., Jr. and V.A. Najjar, *Congenital familial nonhemolytic jaundice with kernicterus.* Pediatrics, 1952. **10**(2): p. 169-80.
2. Arias, I.M., et al., *Chronic nonhemolytic unconjugated hyperbilirubinemia with glucuronyl transferase deficiency. Clinical, biochemical, pharmacologic and genetic evidence for heterogeneity.* Am J Med, 1969. **47**(3): p. 395-409.
3. Tu, Z.H., et al., *Liver transplantation in Crigler-Najjar syndrome type I disease.* Hepatobiliary Pancreat Dis Int, 2012. **11**(5): p. 545-8.
4. Lysy, P.A., et al., *Liver cell transplantation for Crigler-Najjar syndrome type I: update and perspectives.* World J Gastroenterol, 2008. **14**(22): p. 3464-70.
5. Hafkamp, A.M., et al., *Orlistat treatment of unconjugated hyperbilirubinemia in Crigler-Najjar disease: a randomized controlled trial.* Pediatr Res, 2007. **62**(6): p. 725-30.
6. van der Veere, C.N., et al., *Current therapy for Crigler-Najjar syndrome type 1: report of a world registry.* Hepatology, 1996. **24**(2): p. 311-5.
7. Fagiuoli, S., et al., *Monogenic diseases that can be cured by liver transplantation.* J Hepatol, 2013. **59**(3): p. 595-612.
8. Junge, N., et al., *Adeno-associated virus vector-based gene therapy for monogenetic metabolic diseases of the liver.* J Pediatr Gastroenterol Nutr, 2015. **60**(4): p. 433-40.
9. Bortolussi, G. and A.F. Muro, *Advances in understanding disease mechanisms and potential treatments for Crigler–Najjar syndrome.* Expert Opinion on Orphan Drugs, 2018. **6**(7): p. 425-439.
10. Mingozzi, F. and K.A. High, *Therapeutic in vivo gene transfer for genetic disease using AAV: progress and challenges.* Nat Rev Genet, 2011. **12**(5): p. 341-55.
11. Nathwani, A.C., et al., *Adenovirus-associated virus vector-mediated gene transfer in hemophilia B.* N Engl J Med, 2011. **365**(25): p. 2357-65.
12. Nathwani, A.C., et al., *Long-term safety and efficacy of factor IX gene therapy in hemophilia B.* N Engl J Med, 2014. **371**(21): p. 1994-2004.

13. George, L.A., et al., *Hemophilia B Gene Therapy with a High-Specific-Activity Factor IX Variant.* N Engl J Med, 2017. **377**(23): p. 2215-2227.
14. Rangarajan, S., et al., *AAV5-Factor VIII Gene Transfer in Severe Hemophilia A.* N Engl J Med, 2017. **377**(26): p. 2519-2530.
15. Miesbach, W., et al., *Gene therapy with adeno-associated virus vector 5-human factor IX in adults with hemophilia B.* Blood, 2018. **131**(9): p. 1022-1031.
16. Bortolussi, G., et al., *Rescue of bilirubin-induced neonatal lethality in a mouse model of Crigler-Najjar syndrome type I by AAV9-mediated gene transfer.* FASEB J, 2012. **26**(3): p. 1052-63.
17. Bortolussi, G., et al., *Life-long correction of hyperbilirubinemia with a neonatal liver-specific AAV-mediated gene transfer in a lethal mouse model of Crigler-Najjar Syndrome.* Hum Gene Ther, 2014. **25**(9): p. 844-55.
18. Seppen, J., et al., *Adeno-associated virus vector serotypes mediate sustained correction of bilirubin UDP glucuronosyltransferase deficiency in rats.* Mol Ther, 2006. **13**(6): p. 1085-92.
19. Ronzitti, G., et al., *A translationally optimized AAV-UGT1A1 vector drives safe and long-lasting correction of Crigler-Najjar syndrome.* Mol Ther Methods Clin Dev, 2016. **3**: p. 16049.
20. Bockor, L., et al., *Repeated AAV-mediated gene transfer by serotype switching enables long-lasting therapeutic levels of hUgt1a1 enzyme in a mouse model of Crigler-Najjar Syndrome Type I.* Gene Ther, 2017. **24**(10): p. 649-660.
21. Ronzitti, G., et al., *A translationally optimized AAV-UGT1A1 vector drives safe and long-lasting correction of Crigler-Najjar syndrome.* Molecular Therapy — Methods & Clinical Development, 2016. **3**: p. 16049.
22. Collaborators, G.H., et al., *Estimates of global, regional, and national incidence, prevalence, and mortality of HIV, 1980-2015: the Global Burden of Disease Study 2015.* Lancet HIV, 2016. **3**(8): p. e361-87.

23. Ayuso, E., F. Mingozzi, and F. Bosch, *Production, purification and characterization of adeno-associated vectors.* Curr Gene Ther, 2010. **10**(6): p. 423-36.
24. Nathwani, A.C., et al., *Self-complementary adeno-associated virus vectors containing a novel liver-specific human factor IX expression cassette enable highly efficient transduction of murine and nonhuman primate liver.* Blood, 2006. **107**(7): p. 2653-61.
25. Gunn, C.K., *Hereditary Acholuric Jaundice in the Rat.* Can Med Assoc J, 1944. **50**(3): p. 230-7.
26. Cornelius, C.E. and I.M. Arias, *Animal model of human disease. Crigler-Najjar Syndrome. Animal model: hereditary nonhemolytic unconjugated hyperbilirubinemia in Gunn rats.* Am J Pathol, 1972. **69**(2): p. 369-72.
27. Sato, H., et al., *Genetic defect of bilirubin UDP-glucuronosyltransferase in the hyperbilirubinemic Gunn rat.* Biochem Biophys Res Commun, 1991. **177**(3): p. 1161-4.
28. Davidoff, A.M., et al., *Sex significantly influences transduction of murine liver by recombinant adeno-associated viral vectors through an androgen-dependent pathway.* Blood, 2003. **102**(2): p. 480-8.
29. McCarty, D.M., P.E. Monahan, and R.J. Samulski, *Self-complementary recombinant adeno-associated virus (scAAV) vectors promote efficient transduction independently of DNA synthesis.* Gene Ther, 2001. **8**(16): p. 1248-54.
30. Manno, C.S., et al., *Successful transduction of liver in hemophilia by AAV-Factor IX and limitations imposed by the host immune response.* Nat Med, 2006. **12**(3): p. 342-7.
31. D'Avola, D., et al., *Phase I open label liver-directed gene therapy clinical trial for acute intermittent porphyria.* J Hepatol, 2016.
32. Martino, A.T., et al., *The genome of self-complementary adeno-associated viral vectors increases Toll-like receptor 9-dependent innate immune responses in the liver.* Blood, 2011. **117**(24): p. 6459-68.

33. Chahal, P.S., et al., *Production of adeno-associated virus (AAV) serotypes by transient transfection of HEK293 cell suspension cultures for gene delivery.* J Virol Methods, 2014. **196**: p. 163-73.

34. Wright, J.F., *AAV empty capsids: for better or for worse?* Mol Ther, 2014. **22**(1): p. 1-2.

35. Mingozzi, F., et al., *Overcoming preexisting humoral immunity to AAV using capsid decoys.* Sci Transl Med, 2013. **5**(194): p. 194ra92.

36. Nass, S.A., et al., *Universal Method for the Purification of Recombinant AAV Vectors of Differing Serotypes.* Mol Ther Methods Clin Dev, 2018. **9**: p. 33-46.

37. Burnham, B., et al., *Analytical Ultracentrifugation as an Approach to Characterize Recombinant Adeno-Associated Viral Vectors.* Hum Gene Ther Methods, 2015. **26**(6): p. 228-42.

38. Favaro, P., et al., *Host and vector-dependent effects on the risk of germline transmission of AAV vectors.* Mol Ther, 2009. **17**(6): p. 1022-30.

39. Paneda, A., et al., *Effect of adeno-associated virus serotype and genomic structure on liver transduction and biodistribution in mice of both genders.* Hum Gene Ther, 2009. **20**(8): p. 908-17.

40. Davidoff, A.M., et al., *Comparison of the ability of adeno-associated viral vectors pseudotyped with serotype 2, 5, and 8 capsid proteins to mediate efficient transduction of the liver in murine and nonhuman primate models.* Mol Ther, 2005. **11**(6): p. 875-88.

41. Mendell, J.R., et al., *Single-Dose Gene-Replacement Therapy for Spinal Muscular Atrophy.* N Engl J Med, 2017. **377**(18): p. 1713-1722.

42. Mingozzi, F., et al., *Modulation of tolerance to the transgene product in a nonhuman primate model of AAV-mediated gene transfer to liver.* Blood, 2007. **110**(7): p. 2334-41.

43. Montenegro-Miranda, P.S., et al., *Mycophenolate mofetil impairs transduction of single-stranded adeno-associated viral vectors.* Hum Gene Ther, 2011. **22**(5): p. 605-12.

44. Snyder, R.O., et al., *Efficient and stable adeno-associated virus-mediated transduction in the skeletal muscle of adult immunocompetent mice.* Hum Gene Ther, 1997. **8**(16): p. 1891-900.

45. Thummel, C., R. Tjian, and T. Grodzicker, *Construction of adenovirus expression vectors by site-directed in vivo recombination.* J Mol Appl Genet, 1982. **1**(5): p. 435-46.

46. Meliani, A., et al., *Enhanced liver gene transfer and evasion of preexisting humoral immunity with exosome-enveloped AAV vectors.* Blood Adv, 2017. **1**(23): p. 2019-2031.

47. Montenegro-Miranda, P.S., et al., *Adeno-associated viral vector serotype 5 poorly transduces liver in rat models.* PLoS One, 2013. **8**(12): p. e82597.

TABLES

Table 1. GLP toxicology study, biochemistry and hematology data

BIOCHEMISTRY												
	MALES						FEMALES					
	day 8			day 91			day 8			day 91		
ASSAY	VEHICLE	1X	5X	VEHICLE	1X	5X	VEHICLE	1X	5X	VEHICLE	1X	5X
AST (U/L)	90±7	73±12	74±5	85±11	75±8	84±26	78±6	63±5	64±5	70±13	75±9	75±15
ALT (U/L)	78±8	68±14	69±12	59±7	55±7	66±26	53±15	49±9	43±10	53±18	53±13	50±10
ALP (U/L)	280±39	265±43	290±21	103±13	101±15	104±14	190±27	136±32	176±27	61±10	70±16	57±7
GGT (U/L)	2±0	2±0	2±0	2±0	2±0	2±0	2±0	2±0	2±0	2±0	2±0	2±0
CK (U/L)	229±26	238±22	224±36	199±117	136±20	176±63	159±14	193±65	225±20	109±18	129±43	165±75
TBIL (µmol/L)	1.3±0.0	1.3±0.0	1.3±0.0	1.3±0.0	1.3±0.0	1.3±0.0	1.3±0.0	1.3±0.0	1.3±0.0	1.3±0.0	1.3±0.0	1.3±0.0
UREA (mmol/L)	5.1±0.6	4.3±0.1	4.0±0.3	5.4±0.8	5.2±0.6	4.8±0.4	4.4±0.3	4.6±0.3	3.8±0.5	5.1±0.8	5.0±0.8	5.2±0.3
CREAT (µmol/L)	23±1	21±2	16±6	31±4	30±2	29±3	24±2	23±3	26±5	35±4	36±2	35±3
GLUC (mmol/L)	8.58±1.17	18.81±2.91	11.82±2.33	9.65±1.56	9.45±1.91	9.80±2.14	8.67±0.48	10.32±1.14	10.71±1.17	9.18±0.78	9.34±0.85	9.54±1.52
CHOL (mmol/L)	2.2±0.4	2.1±0.9	2.1±0.3	1.5±0.2	1.6±0.3	1.7±0.4	1.9±0.3	2.0±0.6	1.8±0.3	1.8±0.4	1.9±0.4	1.7±0.4
TRIG (mmol/L)	1.19±0.35	1.01±0.38	1.43±0.42	1.18±0.51	1.25±0.38	1.44±0.49	0.44±0.13	0.86±0.44	0.61±0.23	0.83±0.27	0.94±0.43	0.77±0.21
TPROT (g/L)	54±2	54±2	54±1	59±2	60±2	62±1	57±2	57±2	56±3	65±3	68±4	67±4
ALB (g/L)	41±2	40±3	40±1	41±2	42±1	41±2	45±2	43±2	42±3	50±3	52±3	51±3
GLOB (g/L)	13±1	14±3	13±1	18±2	19±1	21±2	13±1	14±2	13±1	15±2	16±2	16±2
A/G	3.1±0.5	2.9±0.8	3.0±0.2	2.3±0.3	2.2±20.1	2.0±0.2	3.6±0.3	3.3±0.5	3.2±0.3	3.5±0.6	3.4±0.6	3.2±0.4
CA (mmol/L)	2.77±0.08	2.76±0.04	2.74±0.07	2.52±0.11	2.55±0.08	2.60±0.06	2.72±0.07	2.69±0.09	2.68±0.07	2.61±0.08	2.64±0.11	2.62±0.13
PHOS (mmol/L)	2.14±0.25	2.77±0.22	2.54±0.23	1.17±0.21	1.28±0.17	1.11±0.13	2.02±0.11	2.41±0.17	2.69±0.13	1.09±0.26	1.10±0.35	1.01±0.18
NA (mmol/L)	144±1	142±2	143±1	143±1	143±1	143±1	143±2	142±1	141±0	142±1	143±1	143±2
K (mmol/L)	4.5±0.2	4.9±0.4	4.7±0.4	4.4±0.4	4.3±0.2	4.5±0.4	3.9±0.2	4.0±0.1	4.1±0.2	3.8±0.2	3.8±0.4	3.9±0.2
CL (mmol/L)	101±1	100±2	100±1	103±2	103±1	103±2	103±2	101±1	101±1	103±1	104±2	104±3

HEMATOLOGY												
	MALES						FEMALES					
	day 8			day 91			day 8			day 91		
ASSAY	VEHICLE	1X	5X	VEHICLE	1X	5X	VEHICLE	1X	5X	VEHICLE	1X	5X
WBC $x10^9$/L	18.86±1.13	13.7±3.3	14.51±4.93	9.95±3.1	9.49±2.66	10.03±2.54	11.16±3.92	11.39±3.96	10±1.45	5.79±1.19	6.34±1.68	5.93±1.41
NEUT $x10^9$/L	1.6±0.47	1.52±0.6	1.24±0.48	1.22±0.39	1.21±0.45	1.26±0.33	1.17±0.58	0.58*±0.17	0.6±0.19	0.52±0.16	0.65±0.24	0.61±0.2
LYMPH $x10^9$/L	11.86±1.17	11.66±2.6	12.67±4.46	8.28±2.7	7.87±2.4	8.33±2.45	9.62±3.19	12.41±3.75	8.96±1.19	5.01±1.07	5.41±1.52	5.05±1.28
MONO $x10^9$/L	0.31±0.05	0.27±0.11	0.35±0.21	0.21±0.1	0.17±0.09	0.18±0.07	0.16±0.1	0.14±0.03	0.22±0.08	0.11±0.05	0.11±0.04	0.1±0.04
EOS $x10^9$/L	0.31±0.05	0.1±0.01	0.09±0.04	0.13±0.06	0.13±0.04	0.13±0.04	0.09±0.03	0.11±0.04	0.09±0.03	0.1±0.02	0.09±0.04	0.1±0.02
BASO $x10^9$/L	0.06±0.01	0.06±0.04	0.07±0.03	0.03±0.02	0.03±0.02	0.03±0.02	0.04±0.03	0.06±0.03	0.03±0.01	0.02±0.01	0.02±0.01	0.01±0
LUC $x10^9$/L	0.09±0.04	0.09±0.03	0.1±0.05	0.08±0.05	0.09±0.04	0.09±0.03	0.08±0.05	0.1±0.05	0.1±0.03	0.05±0.02	0.06±0.04	0.05±0.01
RBC $x10^{12}$/L	6.35±0.2	6.66*±0.11	6.62*±0.14	8.15±0.37	8.3±0.44	8.48±0.33	6.67±0.18	6.66±0.46	6.51±0.19	7.8±0.16	7.68±0.32	7.74±0.25
HGB g/dL	12.7±0.3	13.2±0.4	13.2±0.3	14.2±0.6	14.4±0.5	14.4±0.5	13±0.4	13.4±0.7	12.7±0.5	14±0.4	14±0.4	14±0.5
HCT L/L	0.397±0.008	0.412±0.015	0.412±0.005	0.438±0.015	0.448±0.013	0.446±0.014	0.392±0.016	0.407±0.021	0.384±0.017	0.425±0.013	0.421±0.014	0.427±0.01
MCV fL	62.4±1.7	61.9±1.6	61.9±0.9	58.8±1.9	54±1.6	52.6±1.2	58.7±1.9	61.2±2.8	59±2.3	54.5±1.7	54.8±0.9	55.2±1.7
MCH pg	19.9±0.5	19.8±0.5	19.9±0.2	17.5±0.5	17.4±0.4	17±0.6	19.5±0.5	20.2±0.8	19.5±0.6	18±0.5	18.2±0.4	18.1±0.4
MCHC g/dL	31.9±0.1	31.9±0.3	32.2±0.6	32.5±0.7	32.2±0.5	32.3±0.5	33.2±0.4	33±0.3	33±0.5	33±0.4	33.2±0.4	32.9±0.5
RDW %	12.5±0.2	13.1±0.5	12.9±0.6	13.6±1.6	13.8±0.9	13.9±0.8	11.8±0.3	11.3±0.2	12.1±0.7	11.5±0.4	11.6±0.3	11.4±0.3
PLT $x10^9$/L	947±123	917±88	878±49	861±186	955±86	830±217	985±28	982±105	972±63	782±84	754±142	803±78
RETIC $x10^9$/L	410.7±38	434±73.6	452.3±91.1	262.4±114.8	256.6±74.9	253.6±58.1	292.6±67	285.4±54.8	329.9±90	172.1±35.7	178.1±34	170.3±37.1

See Material and Methods for details on the design of the GLP toxicology and biodistribution study.
For all parameters, n=5 for day 8 and n=10 for day 91; vehicle group at day 91 n=9.
Data sets are reported as mean ± standard deviation. 1X corresponds to animals injected with $5x10^{12}$ vg/kg of (ss)AAV8-hUGTA1; 5X corresponds to animals injected with $2.5x10^{13}$ vg/kg of (ss)AAV8-hUGTA1
* Significantly different from control group (vehicle), p value ≤0.05 (Dunnet)

Table 2: GLP toxicology study, humoral immune response against AAV8 capsid and hUGT1A1 transgene

Vector dose	Anti-AAV8 capsid binding IgG (mean ± SD; µg/mL)				
	baseline	day 8	day 29	day91	day 182
Low dose	0 ± 0.1	38.9 ± 11.3	539.3 ± 161	709.1 ± 16.8	-
High dose	0.1 ± 0.2	26.9 ± 11.8	631.4 ± 93.4	670.7 ± 39.7	1035.9 ± 470.5

Vector dose	Anti-AAV8 capsid binding IgG (mean ± SD; µg/mL)				
	baseline	day 8	day 29	day91	day 182
Low dose	0.3 ± 0.5	0.5 ± 0.7	2.4 ± 1.3	16.1 ± 11.9	-
High dose	0.1 ± 0.2	0.7 ± 0.5	3.5 ± 4.2	11.7 ± 8.3	11.8 ± 7.7

Detection of humoral response directed against capsid and transgene in rat plasma.
See Material and Methods for details on the design of the GLP toxicology and biodistribution study.

Table 3: Testing of species-specific UGT1A1 transgene immunogenicity

UGT1A1 transgene	Number of animals positive for anti-UGT1A1 IgG / total	
	mice	rats
Human	3/4	2/4
Mouse	0/4	Non tested
Rat	Non tested	0/4

FIGURE LEGENDS

Figure 1. (sc)AAV8-hUGT1A1 and (ss)AAV8-hUGT1A1 vectors comparison.

(A) Schematic representation of the transgene expression cassettes. (ss)AAV8-hUGT1A1 (SS) and (sc)AAV8-hUGT1A1 (SC) cassettes are composed by a liver specific promoter, an intron, a poly-A (pA) and the sequence of human UGT1A1 (hUGT1A1). SC expression cassette contains a truncated ITR (Δtrs) that allows for self-complementary genome packaging. **(B)** Purification profiles of (ss)AAV8-hUGT1A1 (SS) and (sc)AAV8-hUGT1A1 (SC) vectors after ultracentrifugation in cesium chloride gradient. The higher bands contain empty particles and the lower bands contain full particles. **(C-D)** Sedimentation profiles of (ss)AAV8-hUGT1A1 **(C)** and (sc)AAV8-hUGT1A1 **(D)** full particles purified by cesium chloride gradient and subjected to analytical ultracentrifugation. In each graph, the X axis represents the sedimentation coefficient expressed in Svedberg units (S), and the Y axis represents the normalized value of the concentration as a function of S (c(S)) measured by Railegh interference or absorbance at 260 nm. **(E)** Denaturing gel performed on genomic extracts obtained from (sc)AAV8-hUGT1A1 (SC) or (ss)AAV8-hUGT1A1 (SS). Molecular weight (MW) is indicated on the left.

Figure 2. (sc)AAV8-hUGT1A1 and (ss)AAV8-hUGT1A1 vectors have similar efficacy *in vitro* and *in vivo*.

(A) Huh7 cells were transduced with AAV8-GFP, (sc)AAV8-hUGT1A1 or (ss)AAV8-hUGT1A1 at 25000 multiplicity of infection. 72 hours after transduction, microsomal extracts were obtained, separated by SDS-PAGE and analyzed by western blot with UGT1A and GAPDH specific antibodies. Molecular weight (MW) is indicated on the left and quantification of band intensity is reported. **(B-D)** 6-8 week-old Gunn rats were injected with PBS (PBS), $1x10^{12}$ vg/rat of (sc)AAV8-hUGT1A1 (SC) or the same dose of (ss)AAV8-hUGT1A1 (SS). **(B)** Total bilirubin (TB) levels measured in serum at the indicated time points. **(C)** Vector genome copy number (VGCN) per cell measured by qPCR in liver. The graph shows the single

values (dots) and the average values (red line) measured in each group and normalized for the number of copies of titin per sample. Statistical analysis was performed by ANOVA (NS, non-significant; PBS n=5, SC n=5, SS n=10). **(D)** Western blot analysis performed on microsomal extracts from rat livers with UGT1A and actin specific antibodies. Molecular weight (MW) is indicated on the left and quantification of band intensity is reported. **(E)** Bilirubin conjugates measured by HPLC in the bile of 8 week-old Gunn rats injected with $5x10^{11}$ vg/kg of (sc)AAV8-hUGT1A1 (SC, n=6) or (ss)AAV8-hUGT1A1 (SS, n=10). Twelve weeks after injection, animals were sacrificed, and bile was analyzed. The graph shows the percentage of conjugated bilirubin (CB) and unconjugated bilirubin (UCB) measured in bile. The level of unconjugated bilirubin observed in wild-type wistar rats is reported in red (WT).

Figure 3. I*n vitro* and *in vivo* comparison of (ss)AAV8-hUGT1A1 produced in HEK293 cells growing in suspension or adherent.

(A-B) Characterization of AAV8 vector expressing hUGT1A1 produced by triple transfection of HEK293 cells cultured in suspension in medium scale bioreactor (10L) and purified by affinity chromatography (SUSP). **(A)** Suspension-produced vector was loaded in a cesium chloride gradient ultracentrifugated and fractionated in 16 fractions starting from the bottom of the tube. Each fraction was analyzed by SDS-PAGE (lanes 1 to 16) and stained with SYPRO Ruby. Molecular weight is indicated on the right. **(B)** VP3 intensity of each fraction was quantified and the percentage of each fraction was plotted in the graph (VP3 protein). Genome titer was measured in each fraction by qPCR. The percentage was calculated as the number of copies in each fraction divided by the sum of the copies in the whole fractions (Genome) **(C)**. Huh7 cells were transduced with AAV8-GFP (GFP), (ss)AAV8-hUGT1A1 produced in HEK293 cells cultured in adhesion (ADH) or in suspension (SUSP) at 5000, 10000 and 25000 multiplicity of infection (MOI). 72 hours post-transduction, microsomal extracts were obtained, separated by SDS-PAGE and analyzed by western blot with UGT1A and actin antibodies. Molecular weight is indicated on the left. Quantification of band intensity is reported on the right. **(D-G)** *In vivo* comparison in a mouse model of hyperbilirubinemia.

Ugt1a1$^{-/-}$ mice were injected with vehicle (PBS) or 3.3x10^{9} vg/mouse of (ss)AAV8-hUGT1A1 vectors produced in HEK293 cells in adhesion (ADH) or in suspension (SUSP). **(D)** TB levels analyzed 30 days after vector injection. **(E)** Vector genome copy number (VGCN) analysis, **(F)** normalized hUGT1A1 mRNA levels and **(G)** protein expression by Western blot in livers of Ugt1a1$^{-/-}$ mice analyzed 30 days post treatment. Data are reported as mean ± standard deviation. Statistical analyses were performed by ANOVA (*=p<0.05; NS, non-significant; UNTR (PT) n=4, ADH n=4, SUSP n=3).

Figure 4. Non-GLP dose-finding study with large scale-produced (ss)AAV8-hUGT1A1 vector.

(A) Sedimentation profile obtained by analytical ultracentrifugation of (ss)AAV8-hUGT1A1 vector, produced by triple transfection of HEK293 cells in suspension at large scale (150L) and purified by affinity chromatography. The X axis represents the sedimentation coefficient expressed in Svedberg units (S), and the Y axis represents the normalized value of the concentration as a function of S (c(S)) measured by Raleigh interference. **(B-C)** 8 week-old Gunn rats were injected i.v. with PBS (PBS) or (ss)AAV8-hUGT1A1 at indicated doses. Total bilirubin (TB) levels in plasma and vector copy number (VGCN) in liver were assessed 84 days post-injection. **(B)** Median with range of TB levels in plasma are shown. **(C)** TB levels plotted against VGCN in liver. Data from all animals are shown.

Figure 5. Non-GLP dose-finding study of (ss)AAV8-hUGT1A1 vector in adult Ugt1$^{-/-}$ mice.

Ugt1$^{-/-}$ mice were injected as adults with the indicated doses (vg/kg). At 1, 2 and 3 months post-injection mice were bled and TB levels in plasma were analyzed. Nine months post injection mice were sacrificed and molecular analysis were carried out. Plasma bilirubin determination in male **(A)** and female **(B)** Ugt1$^{-/-}$ mice. **(C)** Viral genome copy number (VG/cell) at 9 months post injection in male and female mice treated with different doses of rAAV8-hUGT1A1. **(D)** Western blot analysis of liver total protein extracts at 9 months post

injection. $1x10^{11}$ dose male n=5 and female n=5; $5x10^{11}$ dose male n=3 and female n=2; $1x10^{12}$ dose male n=8 and female n=5; $5x10^{12}$ dose male n=6 and female n=5. **(E, F)** Wistar rats (WT and UGT1A1 deficient rats; n=10) and C57Bl/6 mice (n=10) were injected with $5x10^{12}$ vg/kg of an AAV8 vector expressing human coagulation FIX (hFIX). **(E)** Levels of circulating hFIX were measured by ELISA and reported in the graph. **(F)**. Liver genome copy number analysis performed 2 months after vector injection. Data are shown as genome copy number per cell normalized on titin gene. Statistical analyses were performed by ANOVA (*=p<0.05 as indicated).

Figure 6. (ss)AAV8-hUGT1A1 vector shedding and biodistribution.

(A-D) Male and female Sprague-Dawley rats were injected with $5x10^{12}$ vg/kg (1X) or $2.5x10^{13}$ vg/kg (5X) of (ss)AAV8-hUGT1A1 vector produced in suspension at large scale (200L). Vector shedding in fluids collected from D2 to D29**.** Vector genome copy number detected in serum **(A)** and urine **(B)**. Limit of detection (LOD) and limit of quantification (LOQ) of the assay are indicated. **(C)** Correlation of vector genome copy number and hUGT1A1 mRNA expression in different tissues obtained from animals injected with (ss)AAV8-hUGT1A1 vector at $2.5x10^{13}$ vg/kg. **(D)** hUGT1A1 mRNA expression measured in liver 8, 91 and 182 days after vector injection. Mean ± SD is shown. Statistical analyses were performed by ANOVA (NS, not significant). **(E-F)** In-situ hybridization analysis of hUGT1A1 mRNA in liver **(E)** or ovary **(F)** of rats injected with (ss)AAV8-hUGT1A1 vector at $2.5x10^{13}$ vg/kg. **(G-H)** Male rabbits were injected with $5x10^{12}$ vg/kg of (ss)AAV8-hUGT1A1 vector or PBS. **(G)** Vector genomes were quantified by qPCR in epididymis, testis and liver samples collected at Day 150. Mean ± SD are shown. **(H)** Vector shedding in sperm collected from D3 to D150. Mean ± SD of vector genome copy number detected in sperm are shown. Limit of detection (LOD) and limit of quantification (LOQ) of the assay are indicated.

Figure 7. Assessment of immunogenicity of species-specific UGT1A1 in two animal models of CN.

(A-B) Ugt1$^{-/-}$ mice (P60) were injected i.p. with PBS (UNTR) or (ss)AAV8-UGT1A1 vectors coding for mouse transgene at 1x10^{11} vg/kg, at 5x10^{11} vg/kg or 5x10^{12} vg/kg. **(A)** Plasma bilirubin determination in male and female Ugt1-/- mice after treatment with different doses of AAV8-mUGT1A1 vectors. **(B)** Immunofluorescence analysis of representative liver sections from WT, Ugt1-/- untreated and treated with 5x10^{11} vg/kg vector dose. Rectangles show magnification images shown below. 1x10^{11}dose male n=5 and female n=3; 5x10^{11} dose male n=3 and female n=4; 5x10^{12} dose male n=3 and female n=4 (**C-E)** Eight-week-old Gunn rats were injected i.v. with PBS (UNTR) or 5x10^{12} vg/kg of (ss)AAV8-UGT1A1 vector encoding for human UGT1A1 (hUGT1A1) or rat UGT1A1 (rUGT1A1). **(C)** TB levels in plasma of rats analyzed 186 days post treatment. Data are plotted as mean ± SD. Statistical analyses were performed by ANOVA (NS, not significant)**. (D,E)** Anti-UGT1A1 IgG analyzed 186 days post treatment by ELISA for hUGT1A1 **(D)** or by Western-Blot for rUGT1A1 **(E)**. Rat livers expressing rUGT1A1 (+) or not (-) were loaded. Individual serum of rat treated with (ss)AAV8-rUGT1A1 (green) or commercial anti-UGT1A1 antibody (red) were used to detect UGT1A1 protein.

Figure 8. Corticosteroid treatment in CN animal models does not affect gene transfer efficacy.

(A-B) Gunn rats were injected with PBS (black) or 5x10^{12}vg/kg of (ss)AAV8-UGT1A1 (red) at day 0. One month after the treatment, a 15-day tapering dose of methyl-prednisolone was administered intraperitoneally in half of the rats (grey and pink). Rats were weekly bled and sacrificed 3 months after vector injection. **(A)** Total bilirubin (TB) levels were weekly measured and plotted versus time. Data are expressed as mean ± standard error. The internal bar-chart describes the tapering course of methyl-prednisolone (MePRDL). **(B)** Vector genome copy number (VGCN) per cell was measured by qPCR performed on genomic material extracted from livers of Gunn rats. Values were normalized for the number

of copies of genomic DNA using titin as standard. In the figure are showed the single values measured (small black dots) and the median value for each treatment. **(C-E)** Ugt1$^{-/-}$ mice were injected as adults with the indicated doses (vg/kg). A MePRDL treatment was initiated the day before the injection of the AAV vector and lasted for 5 days at decreasing doses (5.0, 2.5, 1.3, 0.6 and 0.3 mg/kg). At 1, 2 and 3 months post-injection mice where bled and TB levels in plasma where analyzed. Nine months post injection mice where sacrificed and molecular analysis where carried out. **(C)** Experimental strategy. **(D)** TB levels in plasma in male and female Ugt1$^{-/-}$ mice after treatment with different doses (vg/kg) of rAAV8-mUGT1A1 with or without corticosteroids. **(E)** VGCN in male and female mice 9 months post injection. Results are expressed as mean ± SD and individual values are plotted. 1x10^{12} dose male sham n=7, male + MePRDL n=2, female sham n=5 and female + MePRDL n=2; 5x10^{12} dose male sham n=6, male + MePRDL n=3, female sham n=4 and female + MePRDL n=2.

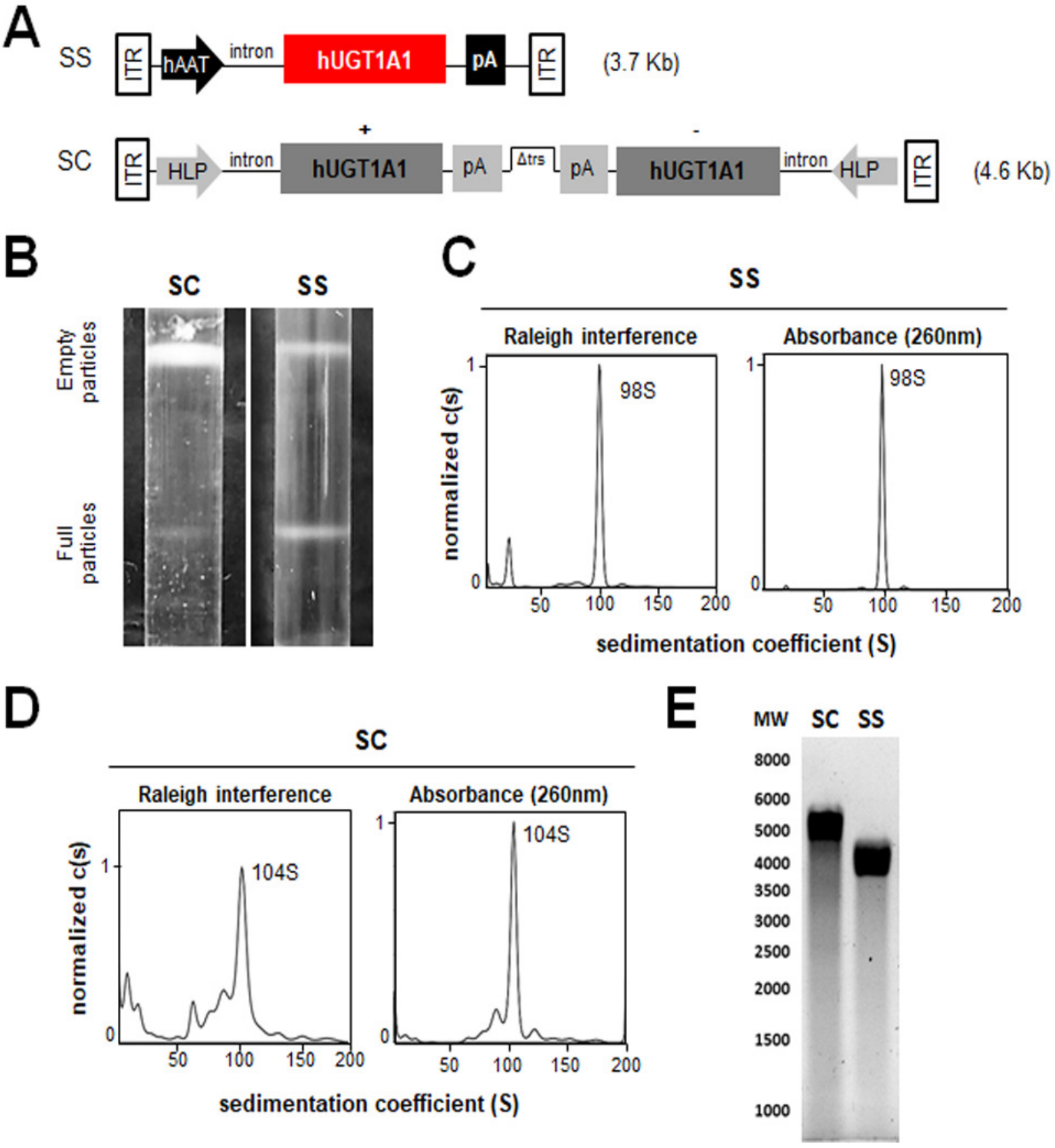
A
SS
ITR
hAAT
intron
hUGT1A1
pA
ITR
(3.7 Kb)
SC
+
-
ITR
HLP
intron
hUGT1A1
pA
Δtrs
pA
hUGT1A1
intron
HLP
ITR
(4.6 Kb)
B
SC
SS
Empty particles
Full particles
C
SS
Raleigh interference
Absorbance (260nm)
98S
98S
normalized c(s)
1
0
50
100
150
200
sedimentation coefficient (S)
D
SC
Raleigh interference
Absorbance (260nm)
104S
104S
normalized c(s)
1
0
50
100
150
200
sedimentation coefficient (S)
E
MW
SC
SS
8000
6000
5000
4000
3500
3000
2500
2000
1500
1000

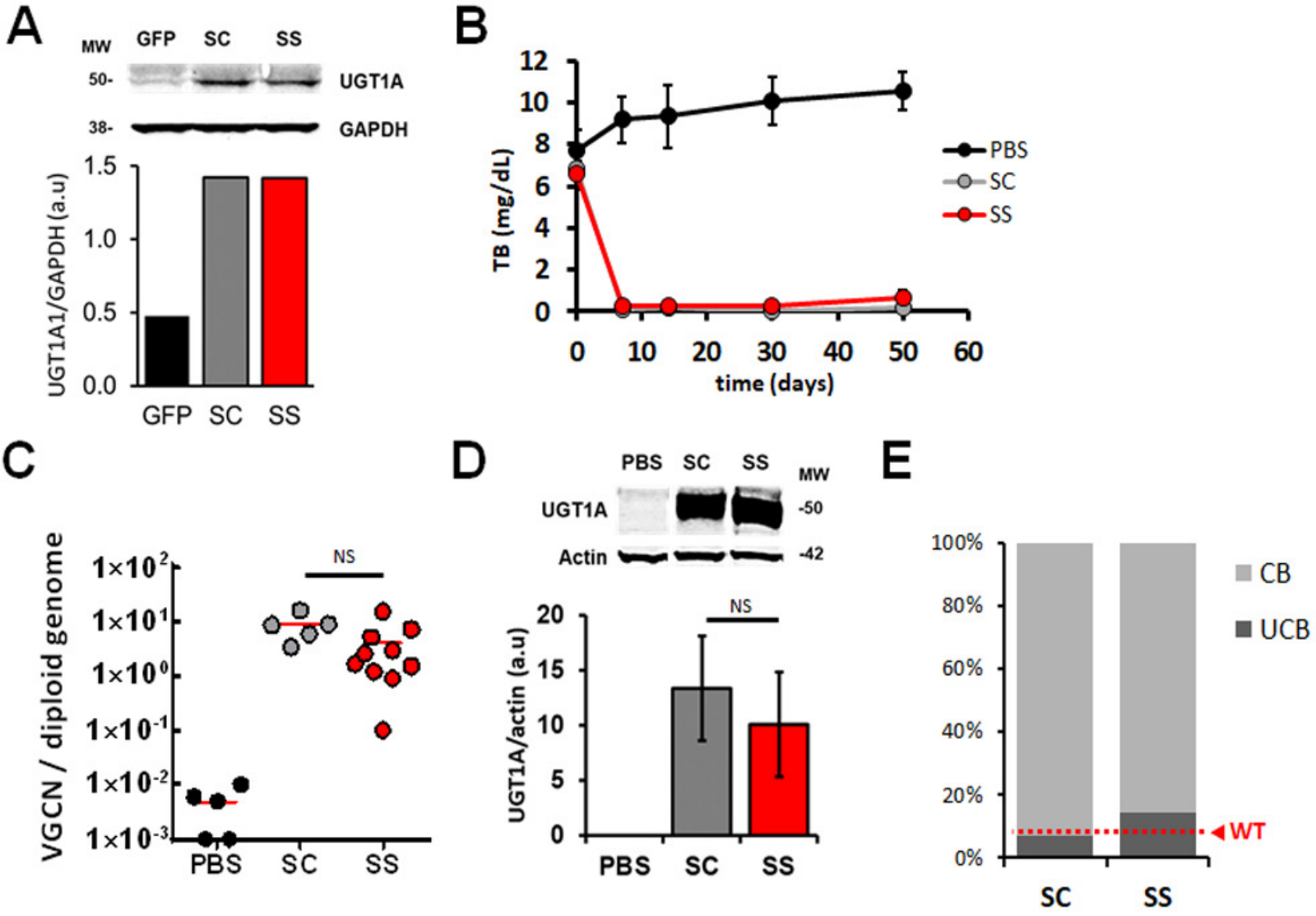
A
MW
GFP
SC
SS
50-
UGT1A
38-
GAPDH
UGT1A1/GAPDH (a.u)
1.5
1.0
0.5
0.0
GFP
SC
SS
B
TB (mg/dL)
12
10
8
6
4
2
0
0
10
20
30
40
50
60
time (days)
PBS
SC
SS
C
VGCN / diploid genome
1×10²
1×10¹
1×10⁰
1×10⁻¹
1×10⁻²
1×10⁻³
NS
PBS
SC
SS
D
PBS
SC
SS
MW
UGT1A
-50
Actin
-42
UGT1A/actin (a.u)
20
15
10
5
0
NS
PBS
SC
SS
E
100%
80%
60%
40%
20%
0%
CB
UCB
WT
SC
SS

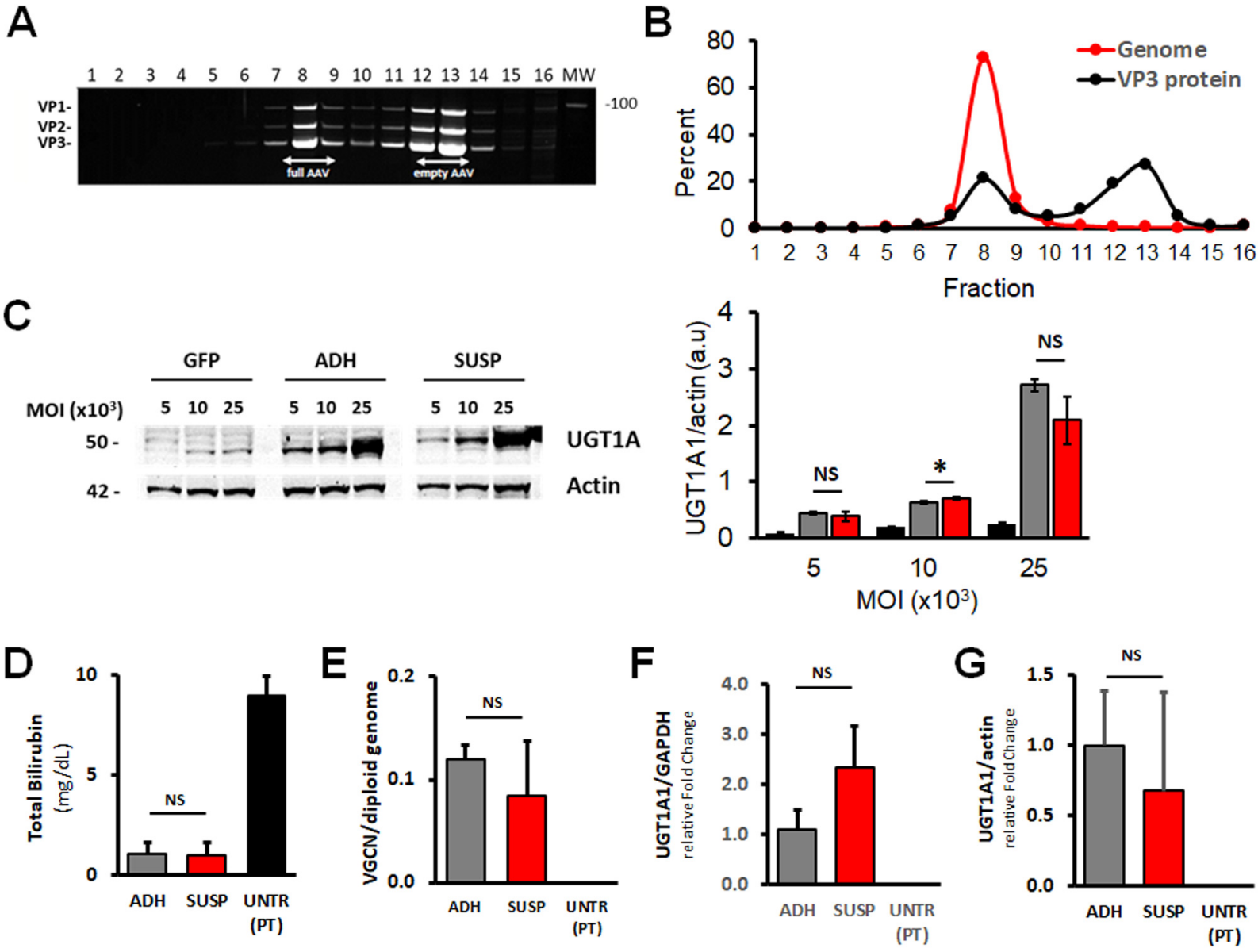
A
1 2 3 4 5 6 7 8 9 10 11 12 13 14 15 16 MW
VP1-
VP2-
VP3-
-100
full AAV
empty AAV
B
Genome
VP3 protein
Percent
Fraction
C
GFP
ADH
SUSP
MOI (x10³)
5 10 25 5 10 25 5 10 25
50 -
42 -
UGT1A
Actin
UGT1A1/actin (a.u)
NS
*
NS
MOI (x10³)
D
Total Bilirubin (mg/dL)
NS
ADH SUSP UNTR (PT)
E
VGCN/diploid genome
NS
ADH SUSP UNTR (PT)
F
UGT1A1/GAPDH relative Fold Change
NS
ADH SUSP UNTR (PT)
G
UGT1A1/actin relative Fold Change
NS
ADH SUSP UNTR (PT)

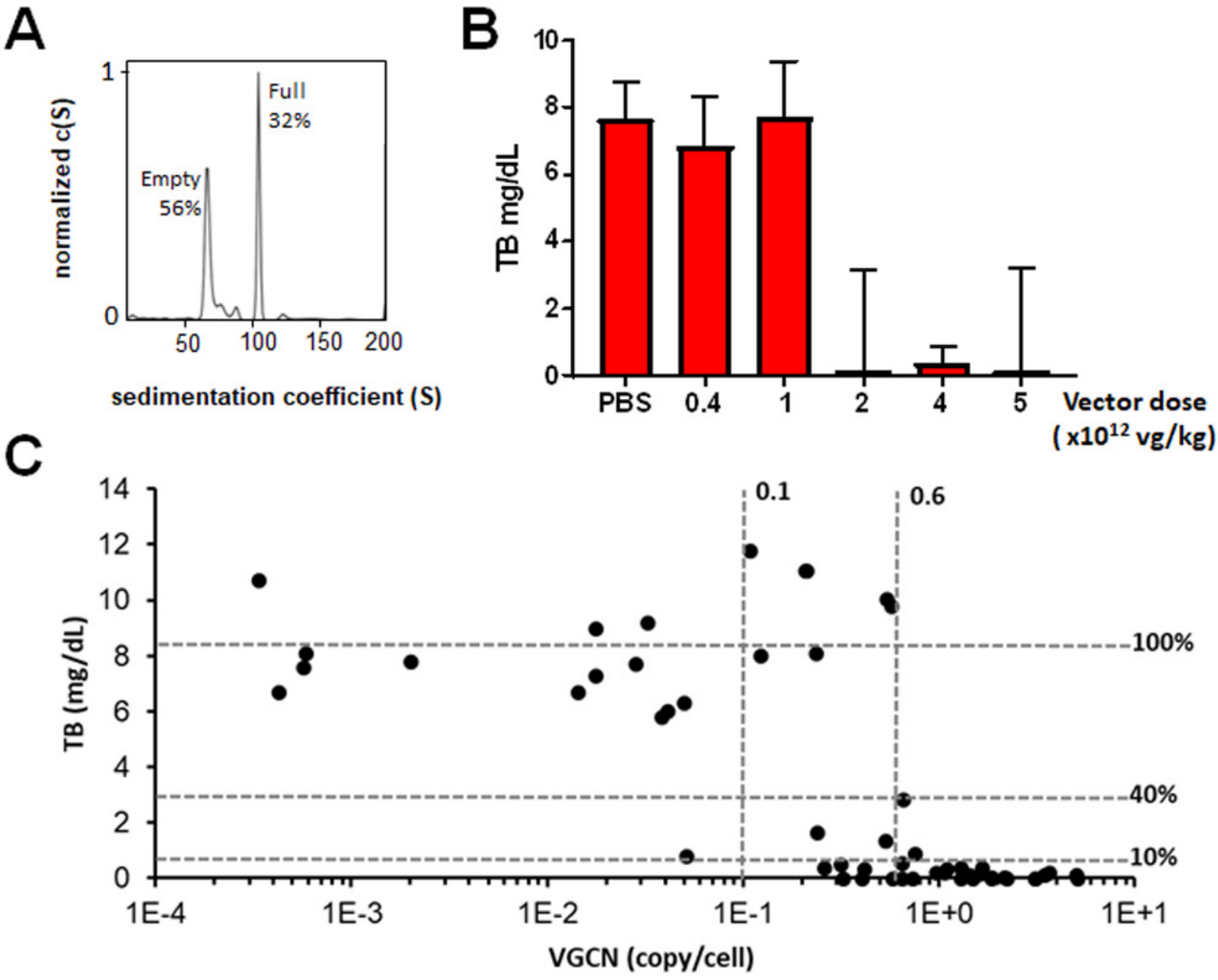
A
normalized c(S)
1
0
Full
32%
Empty
56%
50
100
150
200
sedimentation coefficient (S)
B
TB mg/dL
10
8
6
4
2
0
PBS
0.4
1
2
4
5
Vector dose
(x10^12 vg/kg)
C
TB (mg/dL)
14
12
10
8
6
4
2
0
0.1
0.6
100%
40%
10%
1E-4
1E-3
1E-2
1E-1
1E+0
1E+1
VGCN (copy/cell)

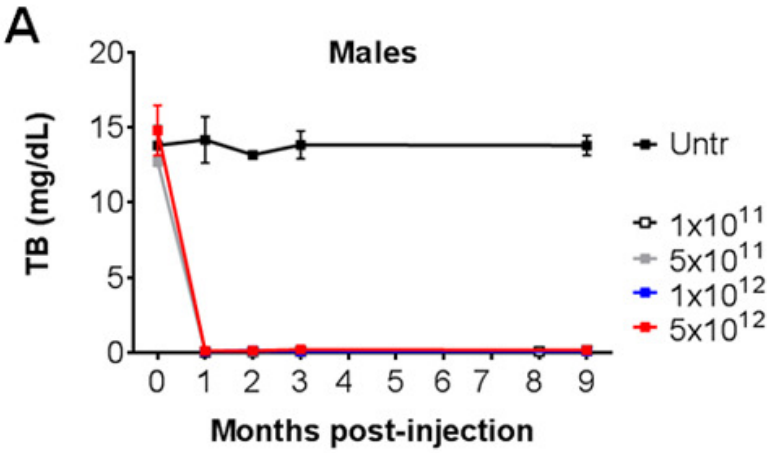
A
Males
TB (mg/dL)
Months post-injection
Untr
1x10^11
5x10^11
1x10^12
5x10^12

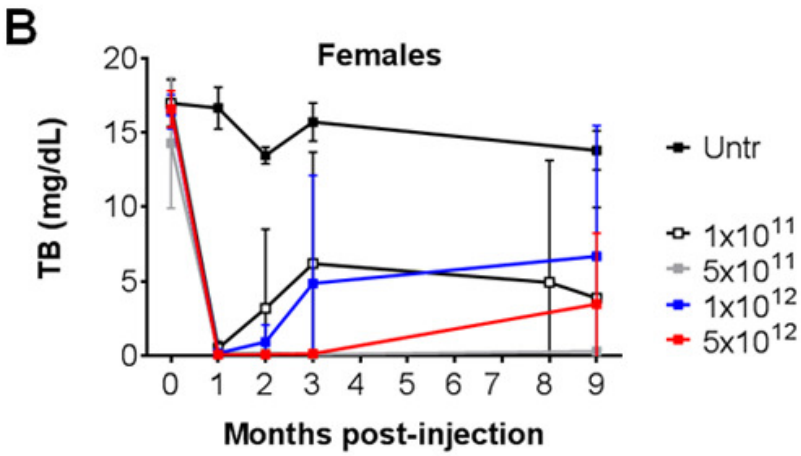
B
Females
TB (mg/dL)
Months post-injection
Untr
1x10^11
5x10^11
1x10^12
5x10^12

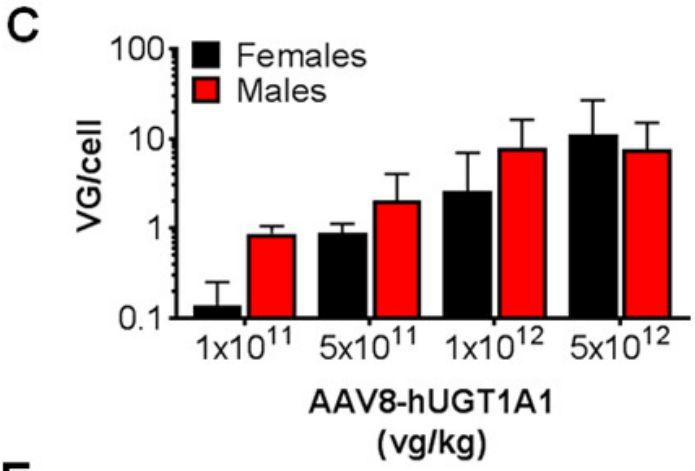
C
Females
Males
VG/cell
1x10^11
5x10^11
1x10^12
5x10^12
AAV8-hUGT1A1
(vg/kg)

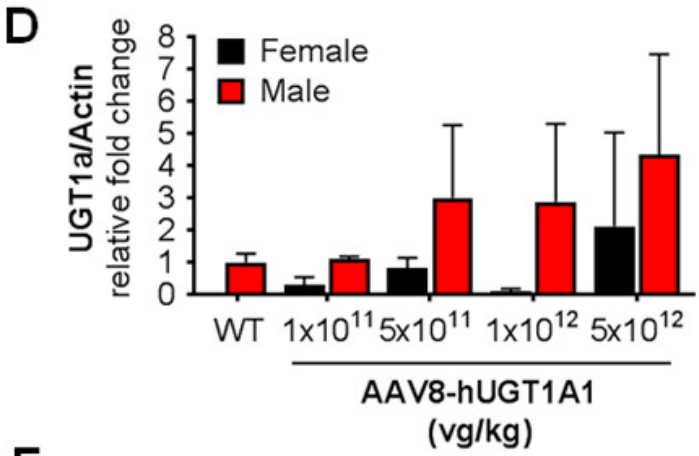
D
Female
Male
UGT1a/Actin
relative fold change
WT
1x10^11
5x10^11
1x10^12
5x10^12
AAV8-hUGT1A1
(vg/kg)

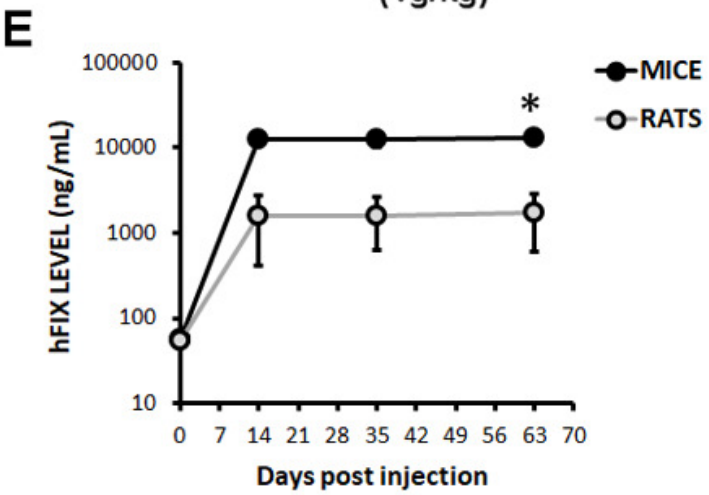
E
MICE
RATS
hFIX LEVEL (ng/mL)
Days post injection

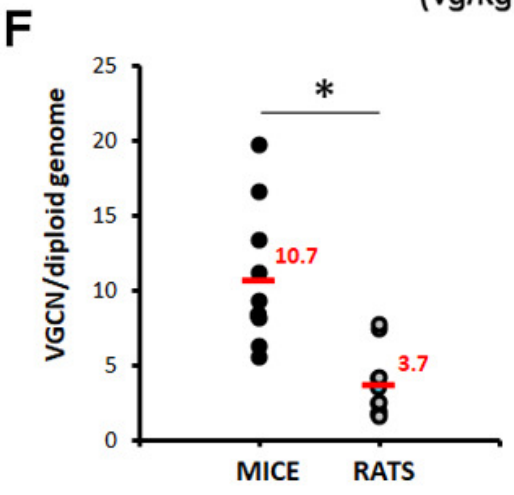
F
VGCN/diploid genome
10.7
3.7
MICE
RATS

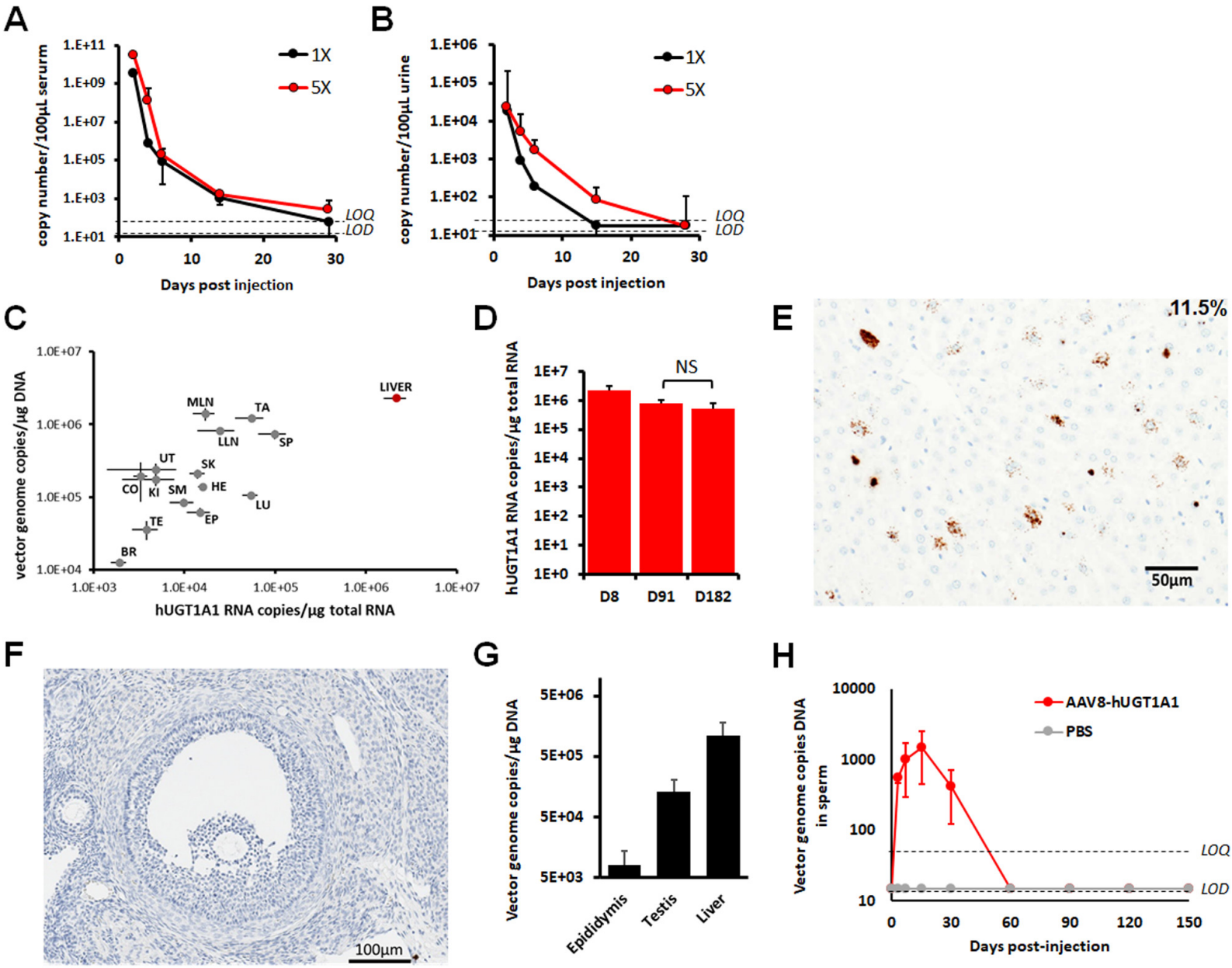
A
1.E+11
1.E+09
1.E+07
1.E+05
1.E+03
1.E+01
copy number/100µL serurm
1X
5X
LOQ
LOD
0
10
20
30
Days post injection
B
1.E+06
1.E+05
1.E+04
1.E+03
1.E+02
1.E+01
copy number/100µL urine
1X
5X
LOQ
LOD
0
10
20
30
Days post injection
C
1.0E+07
1.0E+06
1.0E+05
1.0E+04
vector genome copies/µg DNA
LIVER
MLN
TA
LLN
SP
UT
SK
CO
KI
SM
HE
LU
EP
TE
BR
1.0E+03
1.0E+04
1.0E+05
1.0E+06
1.0E+07
hUGT1A1 RNA copies/µg total RNA
D
hUGT1A1 RNA copies/µg total RNA
1E+7
1E+6
1E+5
1E+4
1E+3
1E+2
1E+1
1E+0
NS
D8
D91
D182
E
11.5%
50µm
F
100µm
G
Vector genome copies/µg DNA
5E+06
5E+05
5E+04
5E+03
Epididymis
Testis
Liver
H
Vector genome copies DNA in sperm
10000
1000
100
10
AAV8-hUGT1A1
PBS
LOQ
LOD
0
30
60
90
120
150
Days post-injection

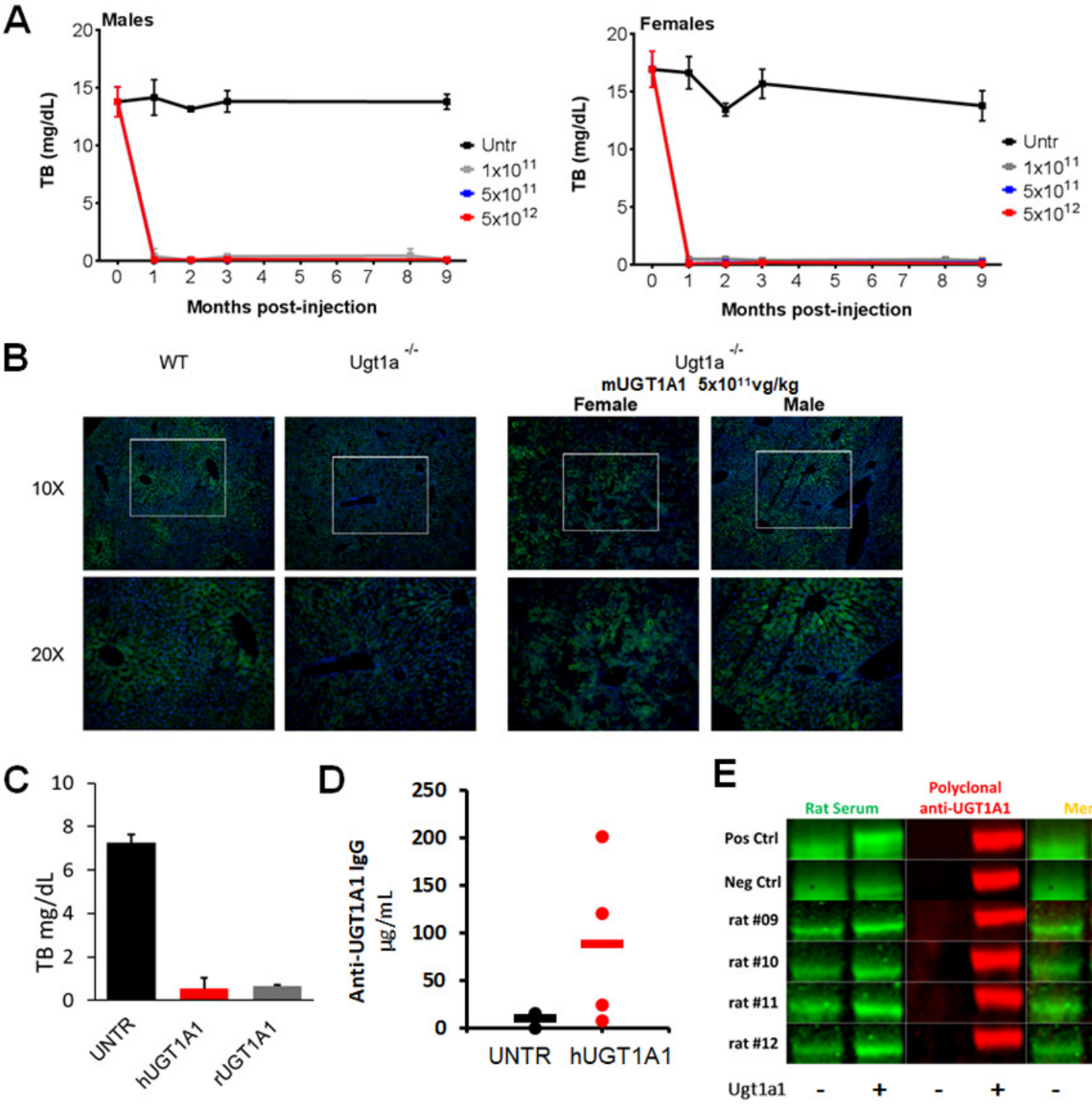
A
Males
TB (mg/dL)
Months post-injection
Untr
1x10^11
5x10^11
5x10^12
Females
B
WT
Ugt1a -/-
Ugt1a -/-
mUGT1A1 5x10^11vg/kg
Female
Male
10X
20X
C
TB mg/dL
UNTR
hUGT1A1
rUGT1A1
D
Anti-UGT1A1 IgG µg/mL
UNTR
hUGT1A1
E
Rat Serum
Polyclonal anti-UGT1A1
Merge
Pos Ctrl
Neg Ctrl
rat #09
rat #10
rat #11
rat #12
Ugt1a1
Aspecific band
Ugt1a1

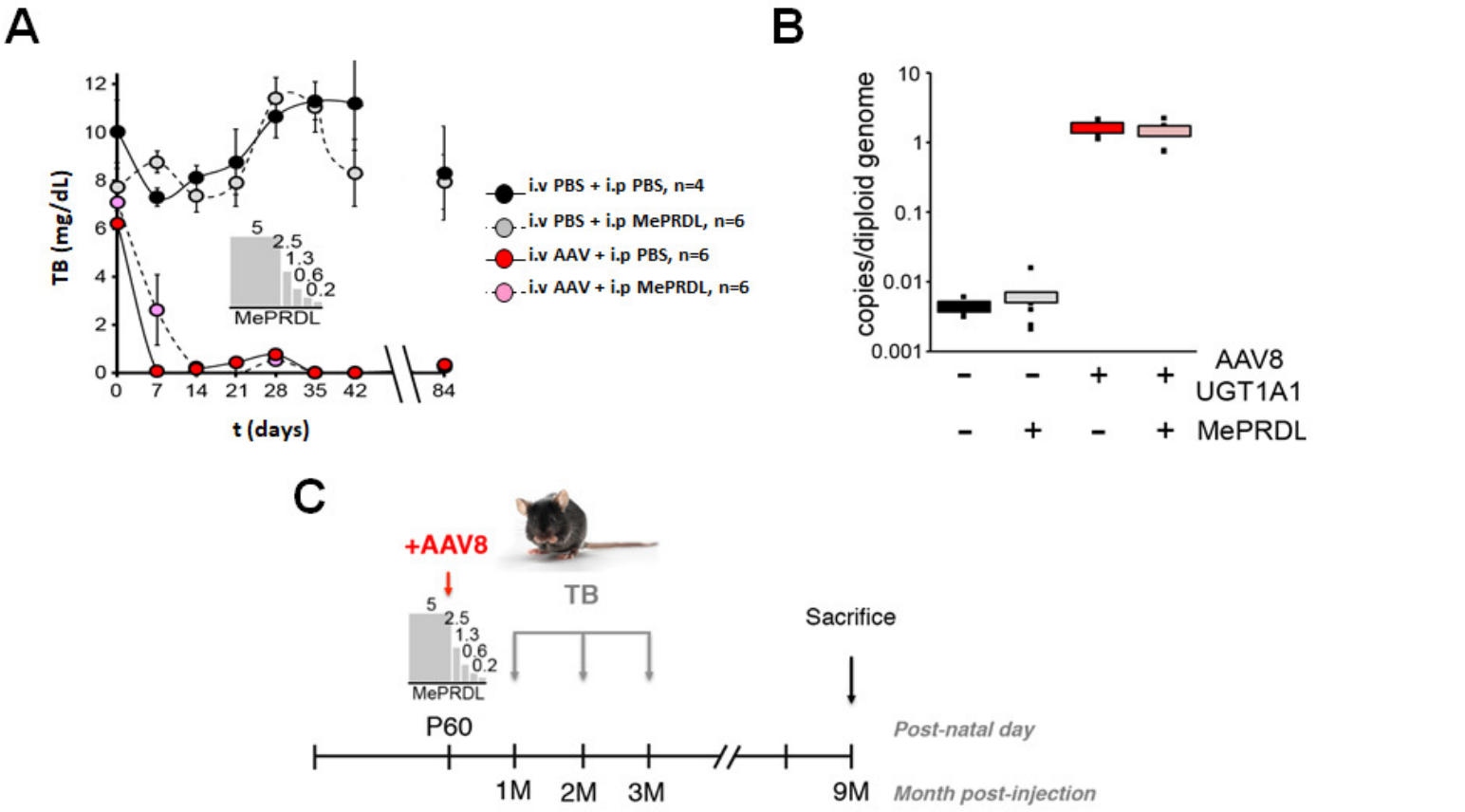
A
TB (mg/dL)
t (days)
MePRDL
i.v PBS + i.p PBS, n=4
i.v PBS + i.p MePRDL, n=6
i.v AAV + i.p PBS, n=6
i.v AAV + i.p MePRDL, n=6
B
copies/diploid genome
AAV8
UGT1A1
MePRDL
C
+AAV8
TB
MePRDL
Sacrifice
P60
Post-natal day
1M
2M
3M
9M
Month post-injection
D
Males
TB (mg/dL)
Months post-injection
Untr sham
Untr +MePRDL
1x10^12 sham
1x10^12 +MePRDL
5x10^12 sham
5x10^12 +MePRDL
Females
TB (mg/dL)
Months post-injection
Untr sham
Untr +MePRDL
1x10^12 sham
1x10^12 + MePRDL
5x10^12 sham
5x10^12 +MePRDL
E
VG/cell
Females
Males
1x10^12
5x10^12
AAV8
UGT1A1
MePRDL